

Confinement from Correlation Functions

Leonard Fister^{1,2} and Jan M. Pawłowski^{2,3}

¹*Department for Mathematical Physics, National University of Ireland Maynooth, Maynooth, Ireland*

²*Institut für Theoretische Physik, Universität Heidelberg, Philosophenweg 16, 69120 Heidelberg, Germany*

³*ExtreMe Matter Institute EMMI, GSI Helmholtzzentrum für Schwerionenforschung mbH, Planckstr. 1, D-64291 Darmstadt, Germany*

We compute the Polyakov loop potential in Yang–Mills theory from the fully dressed primitively divergent correlation functions only. This is done in a variety of functional approaches ranging from functional renormalisation group equations over Dyson–Schwinger equations to two-particle irreducible functionals. We present a confinement criterion that links the infrared behaviour of propagators and vertices to the Polyakov loop expectation value. The present work extends the works of [1–3] to general functional methods and sharpens the confinement criterion presented there. The computations are based on the thermal correlation functions in the Landau gauge calculated in [4–6].

PACS numbers: 12.38.Aw, 11.10.Wx, 11.15.Tk

I. INTRODUCTION

In recent years much progress has been made in our understanding of the strongly-correlated low energy regime of QCD in terms of gauge-fixed correlation functions, for reviews see e.g. [7–14]. This progress is tightly linked to the advancement in our understanding of the basic phenomena of low energy QCD, strong chiral symmetry breaking and confinement. While chiral symmetry breaking allows for a simple description in terms of the related order parameter, the chiral condensate, and its effective potential, our understanding of the confinement-deconfinement phase transition and the mechanism behind is still less developed.

For static quarks with infinite masses, confinement can be thought of in terms of the free energy of a single quark F_q . Removing the antiquark to infinity in a colourless system with a quark-antiquark pair requires an infinite amount of energy in a confined system. The corresponding free energy difference can be related to the free energy of a single quark. Indeed, the gauge field part of such an operator is the Polyakov loop L ,

$$L = \frac{1}{N_c} \text{tr}_f P(\vec{x}), \quad \text{with} \quad P(\vec{x}) = \mathcal{P} e^{ig \int_0^\beta dx_0 A_0(x_0, \vec{x})}, \quad (1)$$

the trace in the fundamental representation of $SU(N_c)$ of the closed Wilson line $P(\vec{x})$ in time direction. Here, \mathcal{P} denotes path ordering, A is the gauge field and the inverse temperature $\beta = 1/T$. The related quark current comprises the worldline of a static quark. The free energy of such a state is proportional to the expectation value of L ,

$$\langle L \rangle \sim \exp^{-F_q/T}. \quad (2)$$

Hence, $\langle L \rangle$ is an order parameter for confinement: it is strictly zero in the confined phase but non-zero in the deconfined phase. This links the confinement-deconfinement phase transition in the Yang–Mills system

to the order-disorder phase transition of center symmetry Z_N in $SU(N_c)$: Under center transformations $z \in Z_N$ the Polyakov loop transforms with $L \rightarrow zL$ in the fundamental representation. We conclude that in the center-symmetric, confining phase we have $\langle L \rangle = 0$, while in the center-broken, deconfined phase we have $\langle L \rangle \neq 0$.

In [1, 2] it has been shown that also $L[\langle A_0 \rangle] \geq \langle L[A_0] \rangle$ for constant fields is an order parameter for static quark confinement. Note that the expectation value $\langle g\beta A_0 \rangle$ relates to the eigenvalues of ϕ with $P(\vec{x}) = \exp i\phi$ and is gauge-invariant and gauge-independent.

The order parameter $L[\langle A_0 \rangle]$ has the advantageous property that its full effective potential $V[A_0]$ can be computed straightforwardly with functional continuum methods. Within the functional renormalisation group (FRG) approach it has been shown [1, 2, 15], that the computation of $V[A_0]$ has a closed representation in terms of the full propagators of gluon, ghosts (and quarks) in constant A_0 -backgrounds. This link of the propagators to the Polyakov loop potential also allowed to put forward a confinement criterion for the infrared behaviour of the ghost and gluon propagators [1].

As similar link of confinement to the infrared behaviour of (gauge-fixed) correlation functions has been put forward more recently with dual order parameters, [15–23]. The latter class of order parameters is directly sensitive to spectral properties of the Dirac operator and hence is tightly linked to quark correlation functions. The former one, $L[\langle A_0 \rangle]$, is directly sensitive to the gluon and ghost correlation functions as well as to the quarks. Nonetheless, there is a close relation between the two classes of order parameters, which has been discussed in [15] for fully dynamical two-flavour QCD at finite temperature. There it has been shown that the two order parameters concur for the case of the dual density or dual pressure.

By now $\langle L[A_0] \rangle$ and the effective Polyakov loop potential $V[A_0]$ has been computed in Yang–Mills theory in the Landau gauge [1, 3, 24], the Polyakov gauge [2] and in the Coulomb gauge [25]. A comparison of $\langle g\beta A_0 \rangle$ in different gauges has been made in [2] which confirms

the formal results of gauge independence. More recently, there have been also first computations of the Polyakov loop potential in Yang-Mills theory on the lattice, see [26, 27]. In [15] the Yang-Mills studies have been extended to fully dynamical two-flavour QCD. In [28, 29] the Polyakov loop potential $V[A_0]$ is used in an effective model approach to QCD with interesting applications to thermodynamic observables.

For a quantitative computation of the Polyakov loop potential, the temperature dependence of the order parameter and in particular the critical temperature a good grip on the thermal ghost and gluon propagators is required. In Landau gauge they have been computed on the lattice, [13, 30–36], and in the continuum, [4–6] with FRG-methods, extending previous studies in extreme temperature limits in the Dyson-Schwinger framework [30, 37–39].

In the present work we compute the Polyakov loop effective potential $V[A_0]$ in the background field formalism [40] in Landau-deWitt gauge within different functional approaches. In Section II we derive representations for the Polyakov loop potential $V[A_0]$ within the FRG-approach, Dyson-Schwinger equations (DSEs) and the two-particle irreducible (2PI-) effective action. In Section III we extend and sharpen the confinement criterion of [1] in terms of the propagators: Infrared suppression of gluons but non-suppression of ghosts suffices to confine static quarks. In Section IV the criterion is applied to general Yang-Mills-matter systems. In Section V the Polyakov loop potential is computed in Yang-Mills theory on the basis of the finite temperature propagators computed within the FRG in [4–6]. The results for the different functional methods are in quantitative agreement in the confinement-deconfinement regime.

II. POLYAKOV LOOP POTENTIAL FROM FUNCTIONAL METHODS

In this section we discuss different representations of the Polyakov loop potential derived from the FRG, DSEs and 2PI-functionals. The Polyakov loop potential V is simply the free energy, or one-particle irreducible (1PI) effective action Γ , evaluated on constant backgrounds A_0 .

A. Polyakov Loop Potential

Most functional approaches are based on closed expressions for the effective action or derivatives thereof in terms of full correlation functions. Hence, the knowledge of the latter in constant A_0 -backgrounds allows us to compute the Polyakov loop potential $V[A_0]$. In turn, confinement requires the Polyakov loop potential to have minima at the confining values for A_0 . In $SU(N_c)$ these are the center-symmetric points. This restricts the infrared behaviour of the correlation functions computed in the constant A_0 -background.

Gauge covariance of the correlation functions and gauge invariance of the effective action and, hence, the effective potential is achieved within the background field approach [40]. We split the gauge field A in a background \bar{A} and fluctuations a about the background, $A = \bar{A} + a$. This split allows us to define background field-dependent gauges that transform covariantly under gauge transformations of both the background and the full gauge field,

$$\bar{D}_\mu a_\mu = 0, \quad \text{with} \quad D_\mu(A) = \partial_\mu - i g A_\mu, \quad (3)$$

and $\bar{D} = D(\bar{A})$. As a consequence all correlation functions transform covariantly under combined gauge transformations of A and \bar{A} . Hence, the effective action Γ is invariant under combined gauge transformations. However, due to the gauge (3) it now depends on the full gauge field A and the background field \bar{A} separately, $\Gamma = \Gamma[\bar{A}; a, c, \bar{c}]$, where c, \bar{c} are the Faddeev-Popov ghosts. The path integral representation is in terms of field-multiplet $\varphi = (a, c, \bar{c})$ and their expectation values $\phi = \langle \varphi \rangle$,

$$e^{-\Gamma[\bar{A}; \phi]} = \int \mathcal{D}\varphi \exp \left\{ -S_A[\bar{A}; \varphi] + \int_x \frac{\delta \Gamma}{\delta \phi} (\varphi - \phi) \right\}. \quad (4)$$

The classical action is given by

$$S_A[\bar{A}; \phi] = \frac{1}{4} \int_x F_{\mu\nu}^a F_{\mu\nu}^a + \frac{1}{2\xi} \int_x (\bar{D}_\mu^{ab} a_\mu^b)^2 + \int_x \bar{c}^a \bar{D}_\mu D_\mu^{ab} c^b, \quad (5)$$

where $F_{\mu\nu}^a$ is the field strength tensor, ξ the gauge fixing parameter and the abbreviation $\int_x = \int_0^\beta dx_0 \int d^3x$. If we now identify the background \bar{A} with the physical background A , the expectation value of the field, we arrive at a gauge invariant effective action

$$\Gamma[A, c, \bar{c}] = \Gamma[A; 0, c, \bar{c}]. \quad (6)$$

The Polyakov loop potential is given by (6) evaluated on a constant A_0 -background, $A_0 = A_\mu \delta_{\mu 0}$,

$$V[A_0^{\text{const}}] := \frac{1}{\beta \mathcal{V}} \Gamma[A_0^{\text{const}}; 0], \quad (7)$$

where \mathcal{V} is the three-dimensional spatial volume. The Polyakov loop, (1), is then evaluated at the minimum $\langle A_0 \rangle := A_{0, \text{min}}$. It has been proven in [1] and [2] that (1) evaluated on the minimum of (7) is an order parameter such as $\langle L[A_0] \rangle \leq L[\langle A_0 \rangle]$.

Functional equations for the effective action can be derived from the FRG, DSEs and 2PI equations. All those equations depend on the correlation functions $\Gamma^{(n)}$ of fluctuation fields a only, schematically given by

$$\Gamma^{(n)}[\bar{A}](p_1, \dots, p_n) = \frac{\delta^n \Gamma[\bar{A}; a]}{\delta a(p_1) \dots \delta a(p_n)} \Big|_{a=0}, \quad (8)$$

where we have suppressed the ghosts and the internal and Lorentz indices. In [1] we have argued that the correlation functions in the background Landau gauge, $\Gamma^{(n)}[\bar{A}]$, are directly related to those in Landau gauge, $\Gamma^{(n)}[0]$. This allows us to use the latter correlation functions within the computation of the effective potential. Here, we recall the argument given in [1] for the ghost and gluon two-point functions, $\Gamma_c^{(2)}, \Gamma_a^{(2)}$, which straightforwardly extends to higher correlation functions:

Gauge covariance of the fluctuation field correlation functions which constrains the difference between $\Gamma^{(n)}[0]$ and $\Gamma^{(n)}[\bar{A}]$. At vanishing temperature the gluon two-point function in Landau gauge splits into four-dimensionally transversal and longitudinal parts with the projection operators

$$\Pi_{\mu\nu}^\perp(p) = \delta_{\mu\nu} - p_\mu p_\nu / p^2, \quad \Pi_{\mu\nu}^\parallel(p) = p_\mu p_\nu / p^2. \quad (9)$$

Hence, the gluon propagator is transversal for all cut-off scales k even though the longitudinal part of the inverse gluon propagator, $\Gamma_A^{(2)}$ receives finite corrections as well.

At non-vanishing temperature we have to take into account chromomagnetic and chromoelectric modes via the respective projection operators P^T and P^L ,

$$\begin{aligned} P_{\mu\nu}^T(p_0, \vec{p}) &= (1 - \delta_{\mu 0})(1 - \delta_{\nu 0})(\delta_{\mu\nu} - p_\mu p_\nu / \vec{p}^2), \\ P_{\mu\nu}^L(p_0, \vec{p}) &= \Pi_{\mu\nu}^\perp(p) - P_{\mu\nu}^T(p_0, \vec{p}), \end{aligned} \quad (10)$$

where $\Pi_{\mu\nu}^\perp$ is the four-dimensional transversal projection operator, see (9). The parameterisation of the gluon and ghost two-point functions in Landau gauge, i.e. the chromoelectric/chromomagnetic gluon $\Gamma_{L/T}^{(2)}$ and the ghost $\Gamma_c^{(2)}$, is then given by, [4–6],

$$\begin{aligned} \Gamma_L^{(2)}(p_0, \vec{p}) &= Z_L(p_0^2, \vec{p}^2) p^2 P^L(p_0, \vec{p}), \\ \Gamma_T^{(2)}(p_0, \vec{p}) &= Z_T(p_0^2, \vec{p}^2) p^2 P^T(p_0, \vec{p}), \\ \Gamma_c^{(2)}(p_0^2, \vec{p}) &= Z_c(p_0, \vec{p}^2) p^2, \end{aligned} \quad (11)$$

where the identity in colour space is suppressed and the wave function renormalisations Z are functions of p_0 and \vec{p} separately. We now parameterise the background field correlation functions in terms of the Landau gauge correlation functions in (11) evaluated at covariant momenta. For the gluon $\Gamma_a^{(2)}$ this gives

$$\begin{aligned} \Gamma_a^{(2)}[A; \phi = 0] &= \sum_{L/T} P^{L/T} (-D^2) Z_{L/T} P^{L/T} \\ &\quad + F_{\rho\sigma}^{cd} f_{\rho\sigma}^{cd}(D) + \Delta m^2(D, A_0), \end{aligned} \quad (12)$$

with non-singular $f(0)$, and where the arguments with respect to the covariant momentum of the projection operators onto the longitudinal and transversal spaces $P_{L/T}(-D_0, -\vec{D})$, respectively, and of $Z_{L/T}(-D_0^2, -\vec{D}^2)$ have been omitted for clarity. Note that the projection operators $P_{L/T}$ do not commute with $Z_{L/T}$ for general

gauge fields. They do, however, for constant gauge fields A_0 . The f -term can not be obtained alone from the Landau-gauge propagator, but is also related to higher Green functions. However, it does not play a rôle for our purpose.

In the computations below we approximate the full inverse gluon propagators by the first line in (12). Similarly the inverse ghost propagator is approximated for constant temporal background A_0 as

$$\Gamma_c^{(2)}[A_0; \phi = 0] \simeq (-D^2) Z_c(D^2). \quad (13)$$

For these backgrounds no f -term as introduced in (12) is present. Note also that a mass term $\Delta m_c^2(0, A_0)$ is kinematically forbidden for the ghost. Hence it can only contribute for momenta larger than zero. As it is subject to the standard thermal decay we neglect it as sub-leading.

B. Thermal Corrections and Critical Scaling

Here we discuss in detail the impact of the neglected thermal corrections Δm^2 . They play a crucial rôle for the correct critical scaling and the value of T_c in the $SU(2)$ -case but is sub-leading in the $SU(3)$ case. This section might be skipped in a first reading as the following results can be understood without it.

We know that $\Delta m^2(D, A_0)$ vanishes at $A_0 = 0$ or $T = 0$. Moreover, the first two terms on the rhs in (12) parameterise all terms in $\Gamma_a^{(2)}$ that only depend on the covariant operator D . At finite temperature, however, the Polyakov loop L is a further invariant, i.e. the Polyakov line, $P(\vec{x})$, cf. (1), transforms covariantly under gauge transformations. These terms are particularly important for the chromoelectric 00 component of the gluon two-point function (12) as they depend on A_0 . Moreover, these terms are not covered by the Landau gauge term in (12) as the related variable is not present for $T = 0$. In addition, $\Delta m^2(D, 0)$ has the standard thermal decay for large momenta p^2 . Hence we shall only discuss it for the low momentum regime, that is $\Delta m^2(0, A_0)$. Note also that (1) is invariant under the periodic gauge transformation $U(t)$ with

$$U(t) = \exp i 2\pi N_c \tau_i t, \quad A_0 \rightarrow A_0 + \frac{2\pi}{\beta g} N_c \tau^i, \quad (14)$$

with τ^i being a generator of the Cartan subalgebra of the respective gauge group, and A_0 in the Cartan subalgebra. This entails that $\Delta m^2(0, A_0)$ is periodic under a shift of A_0 in (14) as is the Polyakov loop potential $V[A_0]$ in (7).

Moreover, the longitudinal correction $\Delta m_L^2(0, A_0)$ is derived from the Polyakov loop potential directly. First we notice that

$$\Delta m_L^2(0, A_0) = \partial_{A_0}^2 V[A_0] - \partial_{A_0}^2 V[0] + \delta m_L^2, \quad (15)$$

where A_0 is the background field in a slight abuse of no-

tation, and δm_L^2 takes care of differences between derivatives with respect to the background A_0 and the fluctuation field a_0 in Δm_L^2 . This term in (15) follows from the Nielsen identity in the background field formalism, [41], in the present context see [42–45]. This identity reads

$$(\partial_{\bar{A}_0} - \partial_{a_0})\Gamma = \frac{1}{2}\text{Tr} \frac{1}{\bar{D}^2} \partial_{\bar{A}_0} \bar{D}^2 - \frac{1}{2}\text{Tr} G_c \partial_{\bar{A}_0} \bar{D}_\mu D_\mu, \quad (16)$$

where both traces only sum over momenta and gauge group indices. The first term in (16) originates in the gauge fixing term, the second one in the ghost term. Indeed the first term on the right hand side is one loop exact, the second term is solely driven by the ghost. Note also that evaluated at $a = 0$, (16) is only non-zero beyond one loop. Applying a further derivative $\partial_{a_0} + \partial_{\bar{A}_0}$ to (16) and evaluating it at $a = 0$ and $D = 0$ relates it to the term δm_L^2 in (15). The Nielsen identity (16) accounts for the different RG-scaling of fluctuation propagators and background propagators and higher correlation functions, as is well-known from perturbative applications. We infer that the projection of (16) on Δm_L^2 guarantees the correct RG-scaling for the second derivative terms of the Polyakov loop potential in (15). This is taken into account by applying the appropriate RG-rescaling, z_a/z_A to the first and second term on the rhs of (15). Here, z_a and z_A are the renormalisation factors of fluctuation field and background field, respectively. Higher order corrections related to the momentum dependence of the RG-scaling which we have neglected in the present discussion due to its thermal decay.

In summary we can estimate Δm_L^2 on the basis of the Polyakov loop potential as

$$\Delta m_L^2 \simeq \frac{z_a}{z_A} (\partial_{A_0}^2 V[A_0] - \partial_{A_0}^2 V[0]). \quad (17)$$

Eq. (17) has the correct periodicity properties and the correct limits. Moreover, it entails that the electric propagator, $(1/\Gamma^{(2)})_L$, carries critical scaling, see also [32]. Note that the latter property does not depend on the present approximation. This also indicates that the electric propagator is enhanced for temperatures $T \lesssim T_c$ as found on the lattice, [13, 30–36]. A careful analysis of the analytic consequences of (16) and (17) will be presented elsewhere. It is left to estimate Δm_T^2 which also has to be proportional to (A_0 -derivatives of) the Polyakov loop potential. In the transversal propagators such terms can only occur together with (covariant) momentum dependencies or powers of the field strength. The latter vanishes for constant temporal backgrounds while the former is thermally suppressed. We conclude that $\Delta m_T^2 \simeq 0$.

We are now in the position to estimate the impact of Δm_L^2 for the $SU(2)$ and $SU(3)$ -computations: It is the electric propagator which directly depends on the Polyakov loop potential. Moreover, this correction is the only term which is directly sensitive to center symmetry. The standard approximations used in functional methods are based on field expansions about vanishing fields

$$\partial_t \Gamma_k[\bar{A}; \phi] = \frac{1}{2} \left(\text{Diagram 1} - \text{Diagram 2} \right)$$

FIG. 1: Functional flow for the effective action. Lines with filled circles denote fully dressed field-dependent propagators (20). Crossed circles denote the regulator insertion $\partial_t R_k$.

and hence are only sensitive to the $su(N_c)$ -algebra. In $SU(2)$ we expect a second order phase transition. Then the critical temperature as well as the correct critical scaling (Ising universality class) are sensitive to the omission of the back-reaction. In the present context this entails that we expect mean-field critical exponents as well as a lowered critical temperature. In $SU(3)$ we expect a first order phase transition and the back-reaction of the Polyakov loop potential is not important for the value of the critical temperature. It should have an impact on the jump of the order parameter which should be increased in the present approximation.

Both expectations are satisfied by the explicit results presented in Section V. It has been also confirmed within the Polyakov gauge that the inclusion of the back-reaction leads to a quantitatively correct critical temperature as well as the expected critical scaling of the Ising universality class for $SU(2)$, see [2]. This has been also confirmed within the Landau gauge, see [46].

C. Flow Equation for the Polyakov Loop Potential

We begin with the FRG representation, which has also been used in [1–3, 24], for QCD-related reviews see e.g. [45, 47–54]. We write the flow equation for the Yang–Mills effective action, $\Gamma_k[\bar{A}; \phi]$, at finite temperature T as

$$\begin{aligned} \partial_t \Gamma_k[\bar{A}; \phi] &= \frac{1}{2} \oint_p (G_a)_{\mu\nu}^{ab}[\bar{A}; \phi](p, p) \partial_t (R_a)_{\nu\mu}^{ba}(p) \\ &\quad - \oint_p (G_c)_{\mu\nu}^{ab}[\bar{A}; \phi](p, p) \partial_t (R_c)_{\nu\mu}^{ba}(p). \end{aligned} \quad (18)$$

where the integration involves the respective gluon and ghost modes. Further, $t = \ln k$, with k being the infrared cut-off scale. The diagrammatic representation given in Fig. 1.

The momentum integration measure at finite temperature is given by

$$\oint_p = T \sum_{n \in \mathbb{Z}} \int \frac{d^3 p}{(2\pi)^3}, \quad \text{with } p_0 = 2\pi T n, \quad (19)$$

where the integration over p_0 turns into a sum over Matsubara frequencies n . Both, gluons and ghosts have periodic boundary conditions, $\phi(x_0 + 1/T, \vec{x}) = \phi(x_0, \vec{x})$, which is reflected in the Matsubara modes $2\pi T n$ with

a thermal zero mode for $n = 0$. Naturally, at vanishing temperature we have $\mathcal{F}_p \rightarrow (2\pi)^{-4} \int d^4 p$. The full field-dependent propagator for a propagation from the fluctuation ϕ_1 to ϕ_2 is given by

$$G_{\phi_1 \phi_2}[\bar{A}; \phi](p, q) = \left(\frac{1}{\Gamma_k^{(2)}[\phi] + R_k} \right)_{\phi_1 \phi_2} (p, q). \quad (20)$$

In short, we use

$$(G_a)^{bc}_{\mu\nu} = G_{a_\mu a_\nu^c}, \text{ and } (G_c)^{ab} = G_{c^a c^b} \quad (21)$$

for the gluon and the ghost propagator, respectively. In (20) we also introduced the regulator function in field space, $R_{k, \phi_1 \phi_2}$, with

$$(R_a)^{bc}_{\mu\nu} = R_{k, a_\mu a_\nu^c}, \quad (R_c)^{ab} = R_{k, c^a c^b} = -R_{k, c^b c^a}. \quad (22)$$

The above entails that (18) only depends on the propagators of the fluctuations ϕ evaluated in a given background \bar{A} . This also holds for the flow of the background effective action $\Gamma_k[\bar{A}; a, c, \bar{c}]$. For more details we refer the reader to [4–6] and Appendix A.

The effective Polyakov loop potential $V[A_0]$ is given by

$$V[A_0] = V_\Lambda[A_0] + \frac{1}{\beta \mathcal{V}} \int_\Lambda^0 dt \partial_t \Gamma_k[A_0], \quad (23)$$

where $V'_\Lambda[A_0] \propto e^{-\Lambda/T} \rightarrow 0$ for sufficiently large $\Lambda/T \gg 1$ and sufficiently smooth regulators, see [4–6]. We conclude that the computation of $V[A_0]$ with FRG-flows only requires the knowledge of the (scale-dependent) propagators $G_{a/c}$, see [1, 3].

D. DSE for the Polyakov Loop Potential

The DSE for Yang–Mills theory relevant for the Polyakov loop potential is that originating in a derivative of the effective action with respect to the A_0 -background at fixed fluctuation. It can be written in terms of renormalised full propagators and vertices and the renormalised classical action. The latter is written as

$$S_{A, \text{ren}}[\bar{A}; \phi] = S_A[z_A^{1/2} \bar{A}; z_\phi^{1/2} \phi; z_g g, 1/z_\xi \xi], \quad (24)$$

with finite wave functions, coupling and gauge parameter renormalisation z_A, z_ϕ, z_g, z_ξ and renormalised fields \bar{A}, ϕ , coupling g and gauge fixing parameter ξ . We have $z_\xi z_a = 1$ due to the non-renormalisation of the gauge fixing term. Moreover, background gauge invariance of the background field effective action (6),

$$D_\mu^{ab} \frac{\delta \Gamma[A; \phi = 0]}{\delta A_\mu^b} = 0, \quad (25)$$

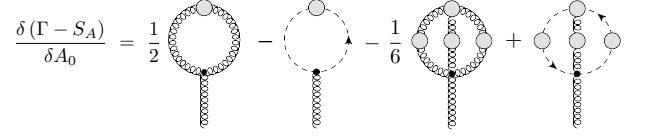


FIG. 2: DSE for the background gluon one-point function.

and non-renormalisation of the ghost-gluon vertex [55, 56] leads to

$$z_g z_A^{1/2} = 1 \quad \text{and} \quad z_g z_a^{1/2} z_c = 1. \quad (26)$$

The above arguments yield the DSE for the Polyakov loop potential, schematically written as

$$\begin{aligned} \frac{\delta(\Gamma[A_0; 0] - S_A[A_0; 0])}{\delta A_0(x)} &= \frac{1}{2} S_{A_0 aa}^{(3)} G_a - S_{A_0 c \bar{c}}^{(3)} G_c \\ &\quad - \frac{1}{6} S_{A_0 aaa}^{(4)} G_a^3 \Gamma_{aaa}^{(3)} + S_{A_0 ac \bar{c}}^{(4)} G_c^2 G_a \Gamma_{ac \bar{c}}^{(3)}, \end{aligned} \quad (27)$$

and the diagrammatic representation given in Fig. 2. In (27) and Fig. 2 we have used the renormalised classical vertices

$$S_{A_0 aa}^{(3)} = z_a \frac{\delta^3 S_A}{\delta A_0 \delta a^2}, \quad S_{A_0 c \bar{c}}^{(3)} = z_c \frac{\delta^3 S_A}{\delta A_0 \delta c \delta \bar{c}}, \quad (28)$$

at $\phi = 0$ and

$$S_{A_0 aaa}^{(4)} = z_g z_a^{3/2} \frac{\delta^4 S_A}{\delta A_0 \delta a^3}, \quad S_{A_0 ac \bar{c}}^{(4)} = \frac{\delta^4 S_A}{\delta A_0 \delta a \delta c \delta \bar{c}}, \quad (29)$$

due to (26). The mixed three-point vertices in (28) have one background leg and two fluctuation legs and differ from the standard vertices: they are A_0 -derivatives of the related fluctuation-field propagator. Using $z_g z_A^{1/2} = 1$ from (26) it follows that the vertices in (28) have renormalisation group properties of fluctuation two-point functions, signaled by z_a and z_c , respectively. The two-point function property also entails that the gluonic vertex contains a piece from the gauge fixing term proportional to $1/\xi$ and the ghost-gluon vertex also involves the gauge field derivative of \bar{D} and not only D .

The mixed four-point vertices in (29) have one background leg and three fluctuation legs and have the renormalisation group properties of the related fluctuation three-point functions multiplied by z_g , signaled by $z_g z_a^{3/2}$ and 1, respectively. The latter follows from $z_g z_a^{1/2} z_c = 1$ in (26). The ghost-gluon four-point function stems from the background field dependence of the Faddeev-Popov operator $-\bar{D}_\mu D_\mu$, and causes an additional two-loop term in the DSE not present in the pure fluctuation DSE.

At asymptotically large momenta the finite wave function renormalisation z_ϕ, z_A are related to the normalisa-

tion of the two point functions with

$$z_\phi = \frac{\Gamma_{\phi\phi}^{(2)}(\mu^2)}{\mu^2} = Z_\phi(\mu^2). \quad (30)$$

Effectively this would amount to using propagators $z_\phi G_{\phi\phi}(p^2)$ with

$$p^2 z_\phi G_\phi(p^2 \rightarrow \infty) \rightarrow 1. \quad (31)$$

Applying the DSE (27) to constant A_0 backgrounds we are finally lead to the DSE equation for the effective Polyakov loop potential with

$$\frac{\partial V[A_0]}{\partial A_0} = \frac{1}{\beta\mathcal{V}} \frac{\partial \Gamma[A_0; 0]}{\partial A_0}, \quad (32)$$

with (27) or Fig. 2 for the right hand side of (32). This equation is similar to the standard DSE for the fluctuation fields with the exception of the two-loop ghost contribution, only the vertices differ. In particular there is a contribution from the gauge fixing vertex which gives a perturbative one-loop contribution to the potential. The external field is a background gluon field with only a temporal component A_0 . This is reflected in the projections, see Appendix B. We conclude that the computation of $V[A_0]$ only requires the knowledge of the propagators and of the full three-point functions $\Gamma_{aaa}^{(3)}$ and $\Gamma_{ac\bar{c}}^{(3)}$ in a constant background.

E. 2PI-Representation for the Polyakov Loop Potential

Now we extend our discussion to the 2PI approach, [57–61], for applications to gauge theories see e.g. [62–74] and the relation to the FRG-approach, see [75, 76]. Its application will simply lead to a convenient resummation scheme for the DSE-equation for the Polyakov loop potential (32) derived in the last chapter: The functional DSE for the effective action displayed in (27) and Fig. 2 follows from the 2PI generating functional

$$\begin{aligned} \Gamma_{2\text{PI}}[G, \bar{A}; \phi] &= S_A[\bar{A}; \phi] - \frac{1}{2} \text{Tr} \log G_a + \text{Tr} \log G_c \\ &\quad - \frac{1}{2} \text{Tr} \Pi_a G_a + \text{Tr} \Pi_c G_c \\ &\quad + \Phi[G, \bar{A}; \phi], \end{aligned} \quad (33)$$

where Φ contains only the 2PI pieces and $\Pi_{a/c} = G_{a/c}^{-1} - S_{a/c}^{(2)}$ are the gluon vacuum polarisation and ghost self-energy, respectively. Here, for the sake of notational simplicity we have set the renormalisation factors $z_{a/c} = 1$. The two-loop diagrams of Φ are displayed in Fig. 3. The 1PI effective action $\Gamma[\bar{A}; \phi]$ is then given with

$$\Gamma[\bar{A}; \phi] = \Gamma_{2\text{PI}}[G[\bar{A}; \phi], \bar{A}; \phi] \quad (34)$$

$$\Phi[G, \bar{A}; \phi] =$$

$$+ \frac{1}{8} \text{diagram} - \frac{1}{12} \text{diagram} + \frac{1}{2} \text{diagram} + \mathcal{O}(\alpha_s^2)$$

FIG. 3: Two-loop diagrams of the 2PI effective action. All propagators are dressed, the full circles denote bare vertices.

with the stationarity condition

$$\left. \frac{\delta \Gamma_{2\text{PI}}}{\delta G} \right|_{G=G[\bar{A}; \phi]} = 0, \quad (35)$$

i.e. the effective action is the 2PI-effective action evaluated on the gap equation. Now we take the derivative w.r.t. A_0 of $\Gamma[\bar{A}; \phi]$ in its 2PI-representation given in (34). The derivative acts on the explicit A_0 -dependence in the classical vertices as well as in the propagators. The latter terms, however, vanish due to the gap equation displayed in (34), thus,

$$\begin{aligned} &\frac{\delta(\Gamma[A_0; 0] - S_A[A_0; 0])}{\delta A_0(x)} \\ &= \left(\text{Tr} \frac{\delta \Gamma_{2\text{PI}}}{\delta G} \frac{\delta G[\bar{A}; \phi]}{\delta A_0} + \frac{\delta \Gamma_{2\text{PI}}[G, \bar{A}; \phi]}{\delta A_0} \right)_{G=G[A_0; \phi]} \\ &= \frac{1}{2} S_{A_0aa}^{(3)} G_a - S_{A_0c\bar{c}}^{(3)} G_c + \left. \frac{\delta \Phi[G, \bar{A}; \phi]}{\delta A_0} \right|_{G=G[A_0; \phi]}, \end{aligned} \quad (36)$$

where, by comparison with (27), Fig. 2, the last term simply is

$$\begin{aligned} &\left. \frac{\delta \Phi[G, \bar{A}; \phi]}{\delta \bar{A}_0} \right|_{G=G[A_0; \phi]} \\ &= -\frac{1}{6} S_{A_0aaa}^{(4)} G_a^3 \Gamma_{aaa}^{(3)} + S_{A_0ac\bar{c}}^{(4)} G_c^2 G_a \Gamma_{ac\bar{c}}^{(3)}. \end{aligned} \quad (37)$$

Eq. (37) can be proven in any order of a given 2PI-expansion scheme such as 2PI perturbation theory or the $1/N$ -expansion. For example, the two-loop terms in Φ , depicted in Fig. 3, provide the right hand side in (37) with classical vertices only. In the present work this is the approximation we shall use for the explicit computations. In any case we conclude that for the present purpose of studying the Polyakov loop potential the 2PI-representation and DSE-representation are quite close and we shall make use of the similarities. Note that this similarity does not hold for e.g. dynamics of a given system where conservation laws such as energy and particle number conservation play a rôle. Then, using self-consistent 2PI-schemes is mandatory.

III. CONFINEMENT CRITERION

The requirement of a confining potential at low temperatures restricts the possible infrared behaviour of low-order correlation functions: The FRG representation of $V[A_0]$ constrains the behaviour of the propagators, and, furthermore, the DSEs and 2PI-equations constrain the three-gluon vertex as well.

First we discuss the restriction of the infrared behaviour of the propagators that follows from the FRG, (18). The present FRG-discussion extends and sharpens the criterion given in [1]. There, the flow equation (18) was rewritten in terms of a total derivative and a term proportional to $\partial_t \Gamma_k^{(2)}$. Schematically this reads

$$\begin{aligned} \partial_t \Gamma_k[\bar{A}; \phi] = & - \oint_p \left(\frac{1}{2} [\partial_t \log G_a]_{\mu\mu}^{aa} - \partial_t [\log G_c]^{aa} \right) \\ & - \oint_p \left(\frac{1}{2} [G_a \partial_t \Gamma_a^{(2)}]_{\mu\mu}^{aa} - [G_c \partial_t \Gamma_c^{(2)}]^{aa} \right). \end{aligned} \quad (38)$$

The second line can be understood as a renormalisation group (RG)-improvement as it is proportional to $\partial_t \Gamma_k^{(2)}$. Moreover, the t -integrals of both lines on the right hand side are independent of the choice of the regulator as the integral of the first line carries this property trivially. In [1] these arguments have been used to drop the second line in (38) as a correction term. This leads to, see [1],

$$\Gamma[\bar{A}; \phi] \simeq - \oint_p \left(\frac{1}{2} [\log G_a]_{\mu\mu}^{aa} - [\log G_c]^a \right) + \Gamma_\Lambda[\bar{A}; \phi]. \quad (39)$$

which reads for the Polyakov loop potential

$$V[A_0] \simeq - \oint_p \left(\frac{1}{2} [\log G_a]_{\mu\mu}^{aa} - [\log G_c]^{aa} \right), \quad (40)$$

as $V'_\Lambda[A_0]$ tends to zero exponentially for large initial cut-off scales Λ . Note also that the approximation (40) has been used in [28, 29]. For confinement at small temperatures, $T \rightarrow 0$, the potential is computed from the small momentum regime with $p^2 \rightarrow 0$ where the propagators are given by $1/(p^{2(1+\kappa)})$ for gluon and ghost with the $T = 0$ scaling exponents κ_a and κ_c , respectively. It has been shown in [1] that confinement enforces

$$d - 2 + (d - 1)\kappa_a - 2\kappa_c < 0, \quad (41)$$

in the approximation (40).

The suppression argument concerning the RG-improvement term presented above was tested in [1]. There, the $T = 0$ -propagators computed in [10] with an optimised regulator have been used. In the spirit of the suppression argument the potential was computed with the $T = 0$ -propagators but with exponential regulator functions which facilitates this specific computation. It has been checked that the RG-improvement term indeed is small. We have now extended the analysis to a fully self-consistent computation with the thermal propagators from [4–6]. Surprisingly, the RG-improvement

term turns out to be large even though it has only a small impact on the phase transition temperature. This relates to the fact that in the non-perturbative regime RG-improvements are not parametrically suppressed by a small coupling and suppression arguments have to be taken with care. This mirrors the 20–30% percent deviation of the standard DSE-results for the $T = 0$ ghost and gluon propagators at about 1 GeV in comparison to lattice results, being linked to the dynamics which drives the phase transition. In the related DSE-approximations the two-loop term in Fig. 2 is dropped. This also implies that related approximation schemes in the 2PI-approach have to be evaluated with care.

Here, we take into account the full flow and note that all loop diagrams in (18) finally boil down to computing

$$T \sum_{n \in \mathbb{Z}} \int_0^\infty \frac{d|\vec{p}|}{(2\pi)^3} \Omega_2 f_k(-D_0^2, \vec{p}^2, A_0), \quad (42)$$

where $\Omega_2 = 4\pi$ is the two-dimensional spherical surface and the dimensionless function f_k is structurally given by

$$f_k = \vec{p}^2 \frac{\partial_t R_k(x)}{x Z(-D_0^2, \vec{p}^2) + \Delta m^2(D, A_0) + R_k(x)}, \quad (43)$$

where $x = -D_0^2 + \vec{p}^2$ and $Z = Z_L, Z_T, Z_c$. In (43) we do not include the overall minus sign of the ghost contribution. The function R_k stands for the respective scalar parts of the regulator functions. The choice of the regulators is at our convenience. For the present discussion (not so much for numerics) it is most convenient to choose Z -independent and $O(4)$ -symmetric regulators,

$$R_k(x) = x r(x/k^2). \quad (44)$$

The terms

$$\Delta m^2(D, 0) = 0, \quad (45)$$

with $\Delta m^2 = \Delta m_L^2, \Delta m_T^2, \Delta m_c^2$, are temperature corrections related to the Polyakov loop. Their impact on the phase transition has been discussed in detail in Section II B. The important property in the present context is their decay with powers of the temperature for $T \rightarrow 0$. At vanishing temperature we regain $O(4)$ -symmetry and $Z(-D_0^2, \vec{p}^2) \rightarrow Z(-D_0^2 + \vec{p}^2)$. In terms of scaling coefficients at vanishing temperature,

$$Z(x) = \mathcal{Z} x^\kappa, \quad (46)$$

the corresponding propagators exhibit non-thermal mass gaps m_{gap} for $\kappa < 0$. Note that the prefactor \mathcal{Z} carries the momentum dimension -2κ . Hence, for $\kappa < 0$ we can ignore Δm^2 in the corresponding propagator for $T/m_{\text{gap}} \rightarrow 0$ as it is suppressed with (potentially fractional) powers of T/m_{gap} . In turn, for propagators with field modes with $\kappa \geq 0$ the temperature correction Δm^2 may play a rôle. However, for the time being we treat

all of them as sub-leading corrections and discuss them later for the field modes with $\kappa > 0$. This amounts to

$$\Delta m^2(D, A_0) \equiv 0, \quad (47)$$

for the present purpose. The integrands in (43) have the limits

$$\lim_{x \rightarrow 0} f_k = 0, \quad \lim_{x \rightarrow \infty} x f_k \rightarrow 0, \quad (48)$$

where we remark that $x = -D_0^2 + \bar{p}^2 \rightarrow 0$ implies both $-D_0^2 \rightarrow 0$ and $\bar{p}^2 \rightarrow 0$. Computing the expression (42) leads to a deconfining potential in A_0 : Taking a derivative w.r.t. A_0 it vanishes at $A_0 = 0$ and the center-symmetric points, i.e. where the Polyakov loop vanishes, $L = 0$. The second derivative is positive at $A_0 = 0$ while it is negative at the center-symmetric points.

Hence, with (47) the single loops in (18) give deconfining potentials. However, the ghost contribution has an overall minus sign. Therefore, the ghost contribution provides a confining potential. This already entails that the Polyakov loop potential in covariant gauges requires the suppression of the gluonic contributions.

In fact the same mechanism is at work in the DSE representation. Restricting ourselves to the one-loop terms for the moment, the gluonic modes give a deconfining potential whereas the ghosts yield a confining contribution. A simple mode counting shows, that the transverse gluons must be suppressed w.r.t. the ghosts for confinement to be present. This is also seen in Appendix B. In other words, with the assumption (47) the necessary condition for confinement is that

$$\lim_{x \rightarrow 0} \frac{1}{Z_{T/L}(x)} = 0 \quad \text{and} \quad \lim_{x \rightarrow 0} \frac{1}{Z_c(x)} > 0, \quad (49)$$

where the second condition guarantees for smooth $Z_c(p)$ that the ghost contribution dominates the trivial contribution of the gauge mode which is precisely $1/2V_{SU(N_c)}$, where $V_{SU(N_c)}$ is the one-loop perturbative potential, see (B5) in Appendix B. In terms of the scaling coefficients introduced in (46) this translates into

$$\kappa_{T/L} < 0 \quad \text{and} \quad \kappa_c \geq 0, \quad (50)$$

where $\kappa_{T/L}$ are the anomalous dimensions of the chromomagnetic and chromoelectric gluon, respectively. Eq. (49) is a sufficient condition for confinement in Yang–Mills propagators (with the assumption (47)) as it leads to a vanishing order parameter, the Polyakov loop expectation value. Note also that it has been shown [77, 78] within a scaling analysis that $\kappa_c \geq 0$ has to hold in the infrared. With this additional information we deduce that (49) encompasses the condition (41) derived in [1]: For the minimal choice $\kappa_c = 0$ we get from (41) the condition $\kappa_a < -(d-2)/(d-1)$ which satisfies (50).

These conditions can be tested in toy models, in which the gluon propagator is suppressed very mildly, whereas the ghost propagator is trivial. This choice is the minimal

satisfaction of the confinement criterion (49). Anticipating the final expressions for the FRG and DSE representations of the Polyakov loop potential, the immanence of confinement at sufficiently low temperatures is shown numerically in Appendix C.

The infrared limits (49) leading to the scaling coefficients (46) are satisfied, as they must, by the existing solutions in the literature, for a detailed overview over the solutions found on the lattice and in the continuum see e.g. [10]. The different solutions vary in the deep infrared. The decoupling solution, found on the lattice and in the continuum, exhibits a trivial ghost and a finite, non-vanishing gluon propagator, where the continuum allows for a scaling solution with a vanishing gluon propagator and an enhanced ghost propagator. In terms of the scaling exponents (46) the decoupling solution translates to $\kappa_a = -1$ and $\kappa_c = 0$, the scaling solution shows $\kappa_c = \kappa = -\kappa_a/2$ with $\kappa \approx 0.595$ [56, 79, 80]. We stress again that both types meet the criterion (50) and exhibit confinement. In the computations presented below we have tested, that the type of solutions does not affect the critical physics at the confinement-deconfinement transition, neither qualitatively nor quantitatively. This is expected, as the relevant range for the phase transition is the mid-momentum region, where both decoupling and scaling solutions agree quantitatively.

We close this section with a discussion of the consequences and implications of (46) and (49): Note first that confinement not only implies a vanishing order parameter but also constrains other observables such as its correlations. The evaluation of these observables in terms of the propagators (and higher vertices) may lead to further, tighter constraints for the propagator. This point of view is interesting for model computations as there the above condition (49) is only a necessary one for deciding whether the model is confining or not. For example, one can easily construct models for Yang–Mills theory that have massive Yang–Mills propagators and a trivial ghost propagator at vanishing temperature. This can be parameterised as

$$G_a(p^2) = \frac{1}{p^2 + m^2}, \quad G_c = \frac{1}{p^2}. \quad (51)$$

Such a combination of propagators leads to a vanishing Polyakov loop expectation value but lacks the necessary positivity violation in the gluon system. It could model Yang–Mills theory in the Higgs phase but not in the confining phase. Note that it is precisely this feature which distinguishes the decoupling solution in Landau gauge Yang–Mills theory with $0 < G_a(0) < \infty$ from a massive solution put down in (51).

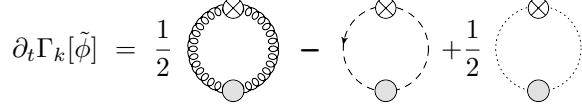


FIG. 4: Functional flow for the effective action of Yang–Mills theory with bosonic matter in the adjoint or fundamental representation, assembled in $\tilde{\phi}$. In either case, the matter fields are represented by the dotted lines adding the third loop.

IV. CONFINEMENT IN YANG–MILLS–MATTER SYSTEMS

The confinement criterion discussed in the last section leads to a simple counting scheme for general theories. In the present section we put it to work in full dynamical QCD with fundamental or adjoint quarks, see e.g. [12, 15, 81, 82], as well as in the Yang–Mills–Higgs system with Higgs field in the fundamental or in the adjoint representation coupled to Yang–Mills theory, formulated in the Landau gauge, e.g. [83–87]. This also serves as a showcase for the general simple counting schemes which has emerged by now.

We concentrate on the one flavour case (Higgs or quark), the generalisation to many flavours is straightforward. Note also in this context that the present confinement criterion constrains the physics properties of a potentially confined phase, it does not prove or disprove its dynamical existence in the theory at hand. For example, it is well-known that for a sufficiently large number of quark flavours in the fundamental or adjoint representation, QCD ceases to be confining. Then the propagators simply do not satisfy the confinement criterion.

We start with a discussion of the adjoint Higgs h (one flavour) with the action

$$S_{\text{Higgs}}[\bar{A}; \phi, h] = S_A + \int_x \text{tr}_{\text{ad}} h^\dagger D_\mu^\dagger D_\mu h + \int_x V(h^\dagger h). \quad (52)$$

The flow equation for the Polyakov loop potential is depicted in Fig. 4. We have already seen that in the Landau gauge the question of a confining potential at low temperatures boils down to counting the massless modes including the prefactors 1 and -2 from the loops of bosons and fermions, respectively, where we normalise the standard boson loop with the prefactor $1/2$ to one. In the symmetric phase at high temperatures, all modes are effectively massless for our counting: All vacuum masses are suppressed with the temperature. Our counting is normalised at the (one-loop) Polyakov loop potential in Yang–Mills theory which is computed from 2 boson loops, that are related to the physical transversal gauge modes; the third transversal contribution and that of the longitudi-

dinal gauge mode are canceled by the ghost contribution,

$$\underbrace{\underbrace{2}_{\text{phys. pol.}} + \underbrace{1}_{\text{transversal}} + \underbrace{1}_{\text{longitudinal}} - \underbrace{2}_{\text{ghost}}}_{\text{gauge bosons}} = 2. \quad (53)$$

Hence, in the present case we have 4 contributions from the gauge field (4 vector modes), -2 ghost contributions (relative factor -2 for the loop), and 1 Higgs contribution. This amounts to an overall factor of 3 for the symmetric phase of the adjoint Yang–Mills–Higgs system,

$$\underbrace{4}_{\text{gauge bosons}} - \underbrace{2}_{\text{ghost}} + \underbrace{1}_{\text{Higgs}} = 3. \quad (54)$$

This has to be compared with the counting factor 2 for the pure Yang–Mills system, leading to the one-loop Polyakov loop potential $V_{SU(N_c)}$ [88, 89], given in Appendix (B5). The one-loop potential for the Yang–Mills–adjoint Higgs system, $V_{\text{ad-h}}$, is hence given by

$$V_{\text{ad-h}}(\varphi) = \frac{3}{2} V_{SU(N_c)}(\varphi). \quad (55)$$

In turn, in the fully-broken phase of the Yang–Mills–Higgs system, we have one radial massive (away from the phase transition) Higgs mode with expectation value h_0 and $N_c^2 - 2$ Goldstone bosons. In the glue sector, $N_c^2 - 2$ gauge bosons acquire an effective mass due to the non-vanishing expectation value of the Higgs field. In the Landau gauge this leads to massive propagators for the $3(N_c^2 - 2)$ transversal modes, if the theory is evaluated at the expectation value of the Higgs field. The gauge mode, even though it also acquires a mass, is effectively massless: Its propagator, evaluated at the expectation value of the Higgs, reads

$$\frac{\xi}{p^2(1 + \xi) + \xi(g h_0)^2} \delta^{ab} \Pi_{\mu\nu}^L(p), \quad (56)$$

and, for Landau gauge, $\xi \rightarrow 0$, it only contributes via the longitudinal part of the regulator proportional to $1/\xi$ in the flow equation or via the gauge-fixing part proportional to $1/\xi$ in the DSE and 2PI formulation. We conclude that the gauge mode in the Landau gauge stays effectively massless in any phase. Together with the remaining massless gauge boson we have $N_c^2 + 2$ massless modes in the gauge boson sector.

For example, in $SU(2)$ we have h^1, h^2, h^3 and without loss of generality we take

$$\langle h^i \rangle = \delta^{i3} h_0, \quad \text{with} \quad V'(h_0^2) = V(h_0^2) = 0, \quad (57)$$

leading to

$$\begin{aligned} S_{\text{Higgs}}[\bar{A}; \phi, h] &= S_A + g^2 h_0^2 \epsilon^{3ab} A_\mu^b \epsilon^{3ac} A_\mu^c \\ &= S_A + (g h_0)^2 [(A_\mu^1)^2 + (A_\mu^2)^2]. \end{aligned} \quad (58)$$

Hence we have $4(N_c^2 - 2) = 8$ massive modes. This includes the gauge mode which, however, is effectively massless in the Landau gauge due to (56). Note that the latter fact is special to Landau gauge. In the unitary gauge also the gauge mode gets massive as does the Faddeev–Popov operator.

We proceed to the Polyakov loop potential. First we note that the massive radial Higgs mode effectively blocks one colour direction with projection operator $\mathcal{P}_{\text{radial}}$. For the transversal gauge field propagators, the situation is exactly the opposite. All the modes in the subspace $\mathbb{1} - \mathcal{P}_{\text{radial}}$ are massive and the massless transversal colour direction is that in direction $\mathcal{P}_{\text{radial}}$. Since we are finally only interested in the sign of the sum of the contribution we simply remark that adding one of the three transversal massless gauge boson contributions to the Higgs effectively restores the Higgs boson contribution in the symmetric regime. We also still have the trivial contribution from the gauge mode. Moreover, the ghost is essentially unchanged as in the pure Yang–Mills case, it still has a massless dispersion. We conclude that due to the relative sign of the ghost contribution the Higgs, the effectively ‘restored’ Higgs contribution and the gauge contribution are canceled by the ghost contribution. This is the manifestation of the Higgs–Kibble mechanism for the Polyakov loop potential in the Landau gauge: The apparently massless contributions cancel each other including those of the Goldstones. In the unitary gauge the Goldstone modes are included in the longitudinal gauge field modes, which would be massive and would have dropped out due to their masses.

What is left is the contribution from the remaining two massless transversal gauge bosons with the colour direction $\mathcal{P}_{\text{radial}}$. For gauge fields A_0 with $\hat{A}_0 \mathcal{P}_{\text{radial}} \neq 0$ or $\mathcal{P}_{\text{radial}} \hat{A}_0 \neq 0$ this provides a deconfining contribution to the Polyakov loop potential which counts as $1/N_c$ in the present counting. Again, all this is apparent in the $SU(2)$ -example. Adding all the massless contributions we arrive at

$$\underbrace{2 + 1/N_c}_{\text{gauge bosons \& Higgs}} - \underbrace{2}_{\text{ghost}} = \frac{1}{N_c}. \quad (59)$$

Hence, the Polyakov loop potential for the Yang–Mills–adjoint Higgs system in the Higgs phase is deconfining, albeit suppressed with order $1/N_c$.

We close the analysis on the Yang–Mills–adjoint Higgs system with a remark on a confining phase in this theory: In this phase all gluon modes are expected to be gapped, except for the gauge mode. Keeping the other modes unchanged, the sum in (59) turns negative implying confinement,

$$\underbrace{1 + 1/N_c}_{\text{gauge bosons \& Higgs}} - \underbrace{2}_{\text{ghost}} = -1 + \frac{1}{N_c}. \quad (60)$$

Note however, that (59) includes gapped Higgs modes. If

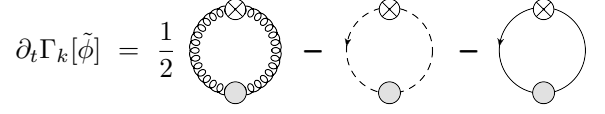


FIG. 5: Functional flow for the effective action of Yang–Mills theory with fermionic matter in the adjoint or fundamental representation, assembled in $\tilde{\phi}$. In either case, the matter fields are represented by the straight lines adding the third loop.

these modes became massless they would counter-balance the gapping of the confined gluons. We conclude that gapped Higgs modes are required in the confined phase. This is reminiscent of the expectation in Yang–Mills–quark systems where one usually expects chiral symmetry breaking in the confined phase.

Let us compare this with the situation in QCD with adjoint fermions. There, the action reads

$$S_{\text{QCD ad}}[\bar{A}; \phi, \psi, \bar{\psi}] = S_A + \int_x \text{tr}_{\text{ad}} \bar{\psi} \not{D} \psi. \quad (61)$$

The flow equation for the Polyakov loop potential is depicted in Fig. 5. The fermionic one-loop contribution to the Polyakov loop potential reads

$$\text{Tr}_{\text{ad+spinor}} \ln \not{D} = \frac{1}{2} \text{Tr}_{\text{ad+spinor}} \ln D_\mu^2 = 4 \frac{1}{2} \text{Tr}_{\text{ad}} \ln D_\mu^2, \quad (62)$$

where we have used that $\not{D}^2 = (D_\mu^2 - 1/2g[\gamma_\mu, \gamma_\nu]F_{\mu\nu})\mathbb{1} = D_\mu^2\mathbb{1}$ for constant fields A_0 , and $\mathbb{1}$ is the identity in spinor space with $\text{tr}_{\text{spinor}}\mathbb{1} = 4$. The fermionic contributions are deconfining as the quarks have anti-periodic boundary conditions, $\psi(t + \beta) = -\psi(t)$, and, hence, the Matsubara frequencies are shifted: $2\pi T(n + 1/2 + \varphi)$. This entails that the Polyakov loop potential is shifted by a factor $1/2$:

$$V_{\text{ad-q}}(\varphi) = -V_{\text{SU}(N_c)}(\varphi + \frac{1}{2}), \quad (63)$$

which is deconfining with the same strength as the Yang–Mills potential. This argument stays valid beyond one loop. For large temperature we conclude that the adjoint quarks for large temperatures lead to $4(N_c^2 - 1)$ contributions,

$$\underbrace{4}_{\text{gauge bosons}} - \underbrace{2}_{\text{ghost}} + \underbrace{4}_{\text{quark}} = 6. \quad (64)$$

This has to be compared with $2(N_c^2 - 1)$ for the pure Yang–Mills system, leading to the one-loop Polyakov loop potential $V_{\text{SU}(N_c)}$, (B5). The one-loop potential for the Yang–Mills–adjoint Higgs system, $V_{\text{ad-h}}$, is hence given by

$$V_{\text{ad-h}}(\varphi) = 3V_{\text{SU}(N_c)}(\varphi). \quad (65)$$

In turn, in the chirally broken phase all quarks are massive and their contributions are removed from the Polyakov loop potential. The glue sector is qualitatively the same as in Yang–Mills theory, the transversal modes are gapped, while the gauge mode is effectively massless. Hence, we are lead to

$$\underbrace{1}_{\text{gauge bosons}} - \underbrace{2}_{\text{ghost}} = -1, \quad (66)$$

the theory is confining in clear contradistinction to the Higgs phase in the Yang–Mills-adjoint Higgs system. Note also that this directly implies *no confinement without chiral symmetry breaking* for QCD with adjoint quarks if the gapping in the quark sector relates to chiral symmetry breaking. Strictly speaking, however, (66) implies *no confinement without gapped quarks*. In turn, in [82] it has been shown that confinement, that is a vanishing expectation value of the Polyakov loop, leads to chiral symmetry breaking. These two results tightly link chiral symmetry breaking and confinement for QCD with adjoint quarks.

In a potential chirally symmetric low energy phase, or better massless low energy phase, we have

$$\underbrace{1}_{\text{gauge bosons}} - \underbrace{2}_{\text{ghost}} + \underbrace{4}_{\text{quark}} = 3, \quad (67)$$

which relates to a deconfining Polyakov loop potential.

We close the section with a discussion of matter in the fundamental representation coupled to Yang–Mills theory. There, center symmetry is explicitly broken. The Polyakov loop is not an order parameter anymore and the question of the confining or Higgs phase has to be answered differently. Indeed, we know that on the lattice these two phases are not well-separated [90–92]. A full discussion of this goes far beyond the aims of the present contribution. Here we simply discuss our counting scheme and compare its outcome for the Yang–Mills-fundamental Higgs system with physical QCD. The action of the Yang–Mills-fundamental Higgs system reads

$$S_{\text{Higgs}}[\bar{A}; \phi, h] = S_A + \int_x \text{tr}_f h^\dagger D_\mu^\dagger D_\mu h + \int_x V(h^\dagger h), \quad (68)$$

similarly to the action for an adjoint Higgs, but with the group trace in the fundamental representation, the Higgs living in the $U(N_c)$. For $SU(2)$, the Higgs is a complex 2×2 -matrix,

$$h = \begin{pmatrix} h_0 + h_3 & h_1 - ih_2 \\ h_1 + ih_2 & h_0 - h_3 \end{pmatrix}. \quad (69)$$

The diagrammatics of the flow equation for the Polyakov loop potential does not change in comparison to the adjoint Higgs and is depicted in Fig. 4, the last loop now involving a trace in the gauge group in the fundamental representation.

The fundamental Higgs has N_c^2 modes due to its

$U(N_c)$ -representation. In the symmetric phase at high temperatures all of them are effectively massless. The group traces, however, are in the fundamental representation of $SU(N_c)$, and, hence, they are suppressed by a factor $1/N_c$ (in the large N_c limit) in comparison to the traces in the adjoint representation. More precisely, the multiplicity of the non-vanishing eigenvalues of A_0 is relatively suppressed with $1/N_c$. The fundamental representation also leads to different eigenvalues of A_0 , see in particular [15]. For example, for $SU(2)$ we have for contributions in the adjoint and fundamental representation

$$V_{\text{fund}}(\varphi) = V_{\text{ad}}(\varphi/2), \quad (70)$$

which can be nicely tested for the one-loop contributions. Note also, that the $U(1)$ -mode h_0 does not couple to the $SU(N_c)$ -gauge field and V_{fund} is a pure $SU(2)$ -potential. In (70) the factor $1/2$ on the right hand side signals the explicit breaking of center symmetry. This also means that one should not simply add the counting factors of contributions in different representations. We merely remark here that as long as the contributions from the center-symmetry breaking sector is small, one may still have a phase transition of the order determined by Z_N -symmetry. The larger the contributions of the center-symmetry breaking sector are, the weaker the transition or finally the cross-over gets. The interpretation of the latter as distinguishing different phases is not clear.

Restricting ourselves to the center-symmetric field modes we get for large temperatures

$$\underbrace{4}_{\text{gauge bosons}} - \underbrace{2}_{\text{ghost}} = 2, \quad (71)$$

the counting of pure Yang–Mills theory. This entails that the Polyakov loop potential of the glue sector is deconfining. At one-loop we have a deconfining total potential,

$$V_{\text{YM-hfund}}(\varphi) = V_{\text{SU}(N_c)}(\varphi) + V_{\text{hfund}}(\varphi). \quad (72)$$

In turn, in the fully-broken phase of the Yang–Mills-fundamental Higgs system we have one radial massive (away from the phase transition) Higgs mode with expectation value h_0 which does not couple to the gauge field. We also have $N_c^2 - 1$ Goldstone bosons. In the glue sector, all $N_c^2 - 1$ gauge bosons acquire an effective mass due to the non-vanishing expectation value of the Higgs field. In the Landau gauge this leads to massive propagators for $3(N_c^2 - 1)$ transversal gauge modes and $N_c^2 - 1$ massless gauge modes. The ghost is massless, and in summary this leads to

$$\underbrace{1}_{\text{gauge bosons}} - \underbrace{2}_{\text{ghost}} = -1, \quad (73)$$

a confining potential for the glue sector. The $N_c^2 - 1$ massless $SU(N_c)$ modes give a center-symmetry breaking potential, which, however, is suppressed by a factor $1/N_c$ for large N_c . Whether for finite N_c one has a cross-over

or still a first order, ($N_c > 2$), or second order, ($N_c = 2$), phase transition is decided dynamically and is not accessible by the present counting. Evidently, however, is the existence of a confining potential in the large N_c -limit. In this limit the pure glue sector dominates the Polyakov loop potential due to the $1/N_c$ -suppression of the Higgs contributions.

Finally we compare the situation in the Yang–Mills–fundamental Higgs system with physical QCD with fundamental quarks, the most interesting and most studied system. Its action is given by

$$S_{\text{QCD}}[\bar{A}; \phi, \psi, \bar{\psi}] = S_A + \int_x \bar{\psi} \mathcal{D} \psi, \quad (74)$$

and the flow equation for the Polyakov loop potential is depicted in Fig. 5. The Higgs in the fundamental representation breaks center symmetry in the same way a fundamental quark does, and the Polyakov loop potential shows no phase transtion. The order parameter $L[\langle A_0 \rangle]$ is a smooth function of temperature similarly to two-flavour QCD studied in [15]. One may be tempted to interpret the behaviour in terms of a cross-over; however, the Wilson loop shows no area law which is in accord with the behaviour of the Polyakov loop. As for the Higgs the pure glue sector shows the counting (73). The part of the potential computed from the massless fermionic modes satisfies

$$\text{Tr}_{\text{f+spinor}} \ln \mathcal{D} = \frac{1}{2} \text{Tr}_{\text{f+spinor}} \ln D_\mu^2 = 2 \text{Tr}_{\text{f}} \ln D_\mu^2, \quad (75)$$

and with anti-periodic boundary conditions for the fermion we get

$$V_{\text{fund-q}}(\varphi) = -2V_{\text{fund}}(\varphi + \frac{1}{2}), \quad (76)$$

where V_{fund} is the potential of one bosonic mode in the fundamental representation. In the large N_c -limit the fermionic contributions are suppressed (unless the number of flavours increases with the number of colours) and yield a confining theory with a first order phase transition. At finite N_c , and in particular $N_c = 2, 3$, we expect a significant influence of the fermions at temperatures above the chiral symmetry breaking scale. Below this scale the fermionic contributions are more and more suppressed and we are left with the pure glue counting.

V. RESULTS FOR THE POLYAKOV LOOP POTENTIAL AND T_c

Here, we compute the Polyakov loop potential within the FRG, DSE and 2PI representation with the propagators at vanishing and finite temperatures obtained from the FRG in [4–6]. There, the finite temperature propagators for all cut-off scales k have been computed on the basis of a given set of propagators at vanishing temperature and vanishing cut-off scale $k = 0$. This minimises

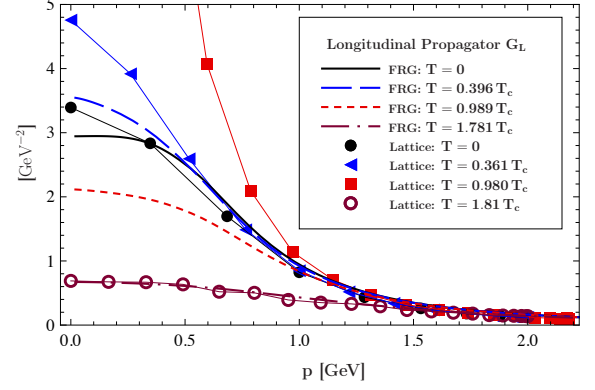


FIG. 6: Zeroth Matsubara mode of the thermal longitudinal gluon propagator from the FRG [4–6] in comparison with lattice results [13, 32].

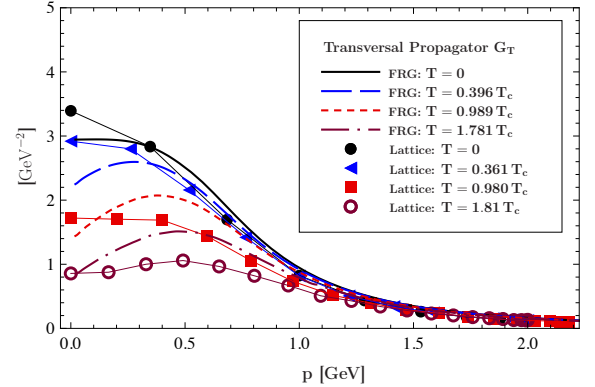


FIG. 7: Zeroth Matsubara mode of the thermal transversal gluon propagator from the FRG [4–6] in comparison with lattice results [13, 32].

the systematic error of a given approximation: Only the difference of the $k=0$ - to the $k \neq 0$ -propagator and the thermal to the $T=0$ -propagator, respectively, is sensitive to the approximation. The results for the Matsubara zero mode for the longitudinal and transversal propagator, $G_{L/T}$, are displayed in Fig. 6 and Fig. 7, respectively, for some temperatures below and above the phase transition. They are compared to lattice results [13, 32]. The FRG results have been obtained in a slightly modified approximation in comparison to [4, 5], see [6]. We resort to the additional approximation

$$Z(p_0^2, \vec{p}^2) \rightarrow Z(0, p_0^2 + \vec{p}^2), \quad (77)$$

which has proven to be an accurate approximation in former studies [6, 30, 31, 39]. For the present purpose of computing the Polyakov loop potential this is a quanti-

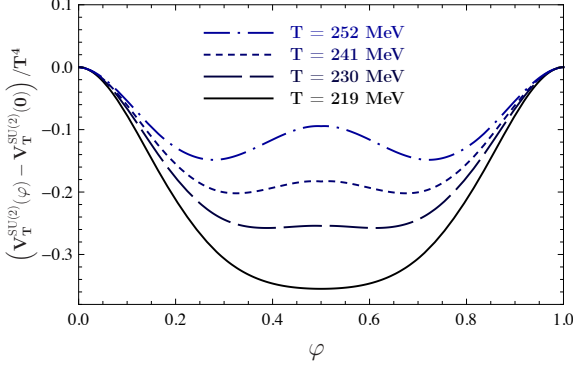


FIG. 8: Polyakov loop potential for $SU(2)$ obtained from the FRG.

tatively reliable approximation as the finite temperature effects in the propagators decay already rapidly for momenta with $p^2/k^2 \gtrsim (2\pi T)^2$ in the FRG computations. We conclude that already the first Matsubara mode is close to the zero mode evaluated as in (77). Note however, that this does not apply to thermodynamical quantities as already pointed out in [4–6], for non-relativistic analogues see [93, 94].

A. Results from the FRG

As discussed before the flow equation has the minimal representation for the Polyakov loop potential as it only requires the propagators in a given background. The present computations improves upon that in [1, 3] with the use of the thermal propagators.

In addition, further emphasis is put on the regulator-independence, see Appendix A. The potential is depicted for temperatures above and below the critical temperature for $SU(2)$ in Fig. 8, and for $SU(3)$ in Fig. 9. Without loss of generality we shift the potential trivially such, that $V(\varphi = 0) = 0$, and divide by the canonical dimension T^4 to simplify the comparison, as the Weiss potential in this normalisation is independent of the temperature.

From these potentials the confinement-deconfinement critical temperatures T_c are determined at

$$T_c^{SU(2)} = 230 \pm 23 \text{ MeV} \quad \text{and} \quad T_c^{SU(3)} = 275 \pm 27 \text{ MeV}. \quad (78)$$

The absolute temperatures in (78) are set in comparison to absolute scales of the lattice propagators with a string tension

$$\sigma = (420 \text{ MeV})^2, \quad (79)$$

which leads to the dimensionless ratios of

$$T_c^{SU(2)}/\sqrt{\sigma} \approx 0.548 \quad \text{and} \quad T_c^{SU(3)}/\sqrt{\sigma} \approx 0.655. \quad (80)$$

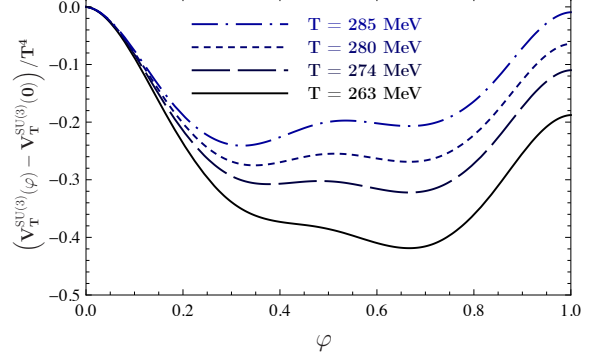


FIG. 9: Polyakov loop potential for $SU(3)$ obtained from the FRG.

For $SU(3)$ our result is in quantitative agreement with the lattice results,

$$T_c^{SU(2)} = 295 \text{ MeV} \quad \text{and} \quad T_c^{SU(3)} = 270 \text{ MeV}, \quad (81)$$

which yield the ratios

$$T_c^{SU(2)}/\sqrt{\sigma} \approx 0.709 \quad \text{and} \quad T_c^{SU(3)}/\sqrt{\sigma} \approx 0.646. \quad (82)$$

For a review on lattice results see e.g. [95]. Our relative normalisation is taken from the peak position of the lattice propagators in [13, 31, 32]. Note however, that this normalisation has an error of approximately 10% which is reflected in the errors in (78).

In turn, for $SU(2)$, the critical temperature $T_c^{SU(2)}$ is significantly lower than the lattice temperature in (81). This is linked to the missing back-reaction of the fluctuations of the Polyakov loop potential, see Section II. Including the back-reaction in the Landau gauge flow leads to a transition temperature of

$$T_c^{SU(2)} = 300 \pm 30 \text{ MeV}, \quad (83)$$

see [46]. More details will be presented elsewhere. This result agrees quantitatively with the lattice temperature as well as with the result obtained with flows in the Polyakov gauge [2] which also reproduced the correct critical scaling of the Ising universality class.

B. Results from DSE & 2PI

The full computation of the Polyakov loop potential (32) from the DSE including the two-loop terms requires the knowledge of the full three-gluon vertex and the full ghost-gluon vertex in the presence of an A_0 -background, see (27) and Fig. 2. Moreover, one has to compute two-loop diagrams in the presence of such a background. Here, we present a simple resummation scheme for ef-

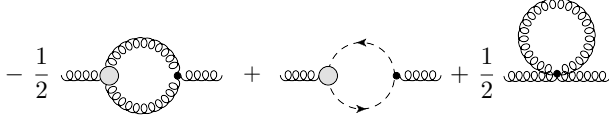


FIG. 10: Gluon vacuum polarisation.

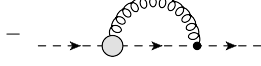


FIG. 11: Ghost self-energy.

fectively computing these terms in an expansion of the Polyakov loop potential in full propagators and full vertices. The simplest way to do this is to consider the 2PI-hierarchy in Fig. 3 up to two-loop. As it also provides some additional information about the resummation scheme we also present a derivation solely within the DSE-approach in Appendix D.

The two-loop terms in Φ can be rewritten in terms of one-loop diagrams with full propagators and gluon vacuum polarisation and ghost self-energy, see Fig. 10 and Fig. 11, respectively. We easily identify the corresponding diagrams in Φ . The first gluonic diagrams in Φ as in Fig. 3 can be rewritten in terms of $(-1/6)$ of the gluonic part of the vacuum polarisation Π_a contracted with the full gluon propagator, which is depicted in Fig. 12.

Then, the last two-loop diagram in Φ , Fig. 3, is rewritten in terms of the missing ghost contribution to the gluonic vacuum polarisation Π_a in Fig. 12, and $(-1/3)$ of the ghost self-energy Π_c contracted with the full ghost propagator, see Fig. 13. Both terms are subtractions to the 1PI-terms $\text{Tr}(-1/2\Pi_a G_a + \Pi_c G_c)$ in the 2PI effective action, (33). This leads to the final form of the effective action,

$$\Gamma[A_0; \phi] = S_A[A_0; \phi] - \frac{1}{2} \text{Tr} \log G_a + \text{Tr} \log G_c \quad (84)$$

$$- \frac{2}{3} \left(\frac{1}{2} \text{Tr} \Pi_a G_a - \text{Tr} \Pi_c G_c \right) + \Delta\Gamma_3[A_0; \phi],$$

with

$$\Delta\Gamma_3[A_0; \phi] = \frac{1}{24} G_a S_{aaaa}^{(4)} G_a + O(\alpha_s^2), \quad (85)$$

comprising the contributions of order α_s^2 in a perturbative 2PI ordering as well as a tadpole contribution. As mentioned before, a derivation of (84) within the DSE-approach can be found in Appendix D. In the explicit computations presented below we will drop $\Delta\Gamma_3$. The tadpole term is set to zero at $T = 0$ in standard renormalisation schemes as it is a mass-contribution. Its thermal A_0 -dependent contribution is suppressed by roughly

$$\frac{1}{8} \text{ (diagram)} - \frac{1}{12} \text{ (diagram)} =$$

$$= \frac{1}{24} \text{ (diagram)} + \frac{1}{6} \left[-\frac{1}{2} \text{ (diagram)} + \frac{1}{2} \text{ (diagram)} \right]$$

FIG. 12: Identification of gluonic part of the vacuum polarisation in the gluonic two-loop diagrams in the 2PI effective action depicted in Fig. 3.

$$\frac{1}{2} \text{ (diagram)} = \frac{1}{6} \text{ (diagram)} + \frac{1}{3} \text{ (diagram)}$$

FIG. 13: Identification of the ghost part of the vacuum polarisation and the ghost self-energy in the ghost-gluon two-loop diagrams in the 2PI effective action depicted in Fig. 3.

one order of magnitude, $1/8$, relative to the contribution of the full tadpole in the final expression, see (84). Moreover, its A_0 -dependent part solely contributes to the $\Delta m^2(0; A_0)$ defined in (15) which we have consistently dropped in the explicit computations presented here.

In conclusion, with $\Delta\Gamma_3 \approx 0$, we have arrived at a representation (84) of the effective action which is manifestly RG-invariant. Indeed, both the first and the second line are separately RG-invariant. One is tempted to even drop the second line in (84) in a first computation. However, even though this should not have a qualitative impact on the phase transition temperature, it turns out to have a big impact on the amplitude of the potential. We have checked this within the flow equation for the Polyakov loop potential: (84) resembles (38). The first lines agree up to the normalisation at $k = \Lambda$ which is trivial. Thus, we deduce that up to the above normalisation the second line of (84) is identical to

$$- \frac{2}{3} \left(\frac{1}{2} \text{Tr} \Pi_a G_a - \text{Tr} \Pi_c G_c \right) + \Delta\Gamma_3[\bar{A}; \phi] \quad (86)$$

$$= - \int_{\Lambda}^0 \frac{dk}{k} \oint_p \left(\frac{1}{2} [G_a \partial_t \Gamma_a^{(2)}]_{\mu\mu}^{aa} - [G_c \partial_t \Gamma_c^{(2)}]^{aa} \right),$$

where the right hand side has the manifest RG-invariance due to being an integrated flow. We have already discussed in Section III below (41) that the integrated flow in (86) is not negligible for the potential even though it does not play a major rôle for the phase transition temperature. We emphasise that a detailed comparison of the different approximations is of great interest

for phenomenological applications in QCD, and in particular also for approaches to QCD within Polyakov-loop enhanced low energy models, see e.g. [96–106]. This analysis is beyond the scope of the present work and will be presented elsewhere.

Hence, we also consider the second line in (84) and use the scheme-independence of the result in (84) to further simplify the computation: With the Dyson equation,

$$G_\phi^{-1} = z_\phi S_\phi^{(2)} + \Pi_\phi, \quad (87)$$

we rewrite the DSE for the effective potential, (32), in terms of the one-loop diagrams in Fig. 2 and the rest,

$$\begin{aligned} \beta \mathcal{V} \frac{\partial V[A_0]}{\partial A_0} &= \frac{1}{2} S_{A_0 aa}^{(3)} G_a - S_{A_0 c\bar{c}}^{(3)} G_c \\ &+ \frac{1}{3} \left(\frac{1}{2} \text{Tr} G_a \frac{\partial \Pi_a}{\partial A_0} - \text{Tr} G_c \frac{\partial \Pi_c}{\partial A_0} \right) \\ &- \frac{2}{3} \left(\frac{1}{2} \text{Tr} \frac{\partial G_a}{\partial A_0} \Pi_a - \text{Tr} \frac{\partial G_c}{\partial A_0} \Pi_c \right). \end{aligned} \quad (88)$$

After performing the Lorenz traces in the second line of (88), the remaining operator traces are simply of the form

$$\text{Tr} \frac{\partial x}{\partial A_0} \frac{Z + x Z' - z}{x Z}, \quad \text{Tr} \frac{\partial x}{\partial A_0} \frac{(Z - z)(Z + x Z')}{x Z^2} \quad (89)$$

where $x = -D^2(A_0)$, $Z = Z(-D_0^2, -\vec{D}^2)$ are the respective wave functions, see (11). The abbreviation Z' stands for the the p_0^2 -derivative of Z ,

$$Z'(-D_0^2, -\vec{D}^2) = \partial_{p_0^2} Z(p_0^2, -\vec{D}^2) \Big|_{p_0^2 = -D_0^2}.$$

Now we minimise the size of the contributions from the second and third line in (88) close to the transition temperature by using an appropriate RG-scheme, that is an appropriate renormalisation scale μ^2 with $z = Z(\mu^2)$ at $T = 0$. Since we are interested in the physics at temperatures at about Λ_{QCD} this already implies $\mu \approx 1$ GeV. We can further restrict this choice by demanding that for $p_0 = 0$ and $A_0 = 0$ we have

$$\begin{aligned} &\left[\frac{1}{2} \frac{Z_a + x Z'_a - z_a}{Z_a} + \frac{(Z_a + x Z'_a)(Z_a - z_a)}{Z_a^2} \right. \\ &\left. - \frac{Z_c + x Z'_c - z_c}{Z_c} - 2 \frac{(Z_c + x Z'_c)(Z_c - z_c)}{Z_c^2} \right]_{x=\mu} = 0. \end{aligned} \quad (90)$$

Eq. (90) minimises the integrand in the momentum integrals in the second and third line in (88) at the momenta with the largest contributions. In (90) a sum over the chromoelectric and the two chromomagnetic polarisations is understood. For temperatures $T \lesssim 200 - 300$

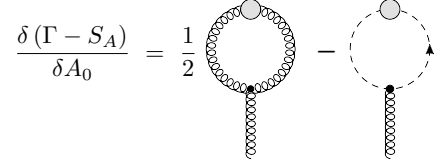


FIG. 14: One-loop truncated DSE for the effective action.

MeV (90) is solved for

$$\mu_{\text{opt}} \approx 1.08 \text{ GeV}. \quad (91)$$

We also can investigate the μ -dependence of the splitting related to the normalisation with z . To that end we apply the related variation to (90), that is the operator $\mu \partial_\mu z_{\phi_i} \partial_{\phi_i}$ and obtain from (90)

$$\left[\frac{1}{2} \eta_{a,0}(3 - \eta_{a,T}) - \eta_{c,0}(3 - \eta_{c,T}) \right]_{x=\mu} = 0, \quad (92)$$

with

$$\eta_{\phi,T}(p^2) = - \frac{p \partial_p Z_\phi(p^2)}{Z_\phi(p^2)}. \quad (93)$$

Again this yields $\mu \approx 1$ GeV which entails that the contribution of the second and third line in (88) can be minimised for temperatures close to T_c along (90). Note also that, since the differences are marginal, it can also be evaluated at $T = 0$ as a first good approximation. There we have $z = Z(\mu^2)$ and (90) simplifies to

$$\left[\frac{1}{2} \frac{Z_a + x Z'_a - z_a}{x Z_a} - \frac{Z_c + x Z'_c - z_c}{x Z_c} \right]_{x=\mu} = 0, \quad (94)$$

which is satisfied for $\mu \approx 1$ GeV as well. The constraint (90) fixes the RG-scale with $\mu_{\text{opt}} = 1.08$ GeV close to Λ_{QCD} and πT_c in the temperature regime between $T = 0 - 300$ MeV. Moreover, it can be shown that a variation of μ in this regime by 100% only leads to changes of the results on the percent level, in particular T_c does not change at all. For the numerical computations we have chosen

$$z_a = Z_a(\mu^2), \quad z_c = Z_c(\mu^2), \quad \text{at} \quad \mu = 1.08 \text{ GeV}. \quad (95)$$

Note that this RG-scheme effectively normalises the propagators used in the DSE and 2PI hierarchy to one at the RG-scale, $z/(\Gamma^{(2)}(\mu^2)/\mu^2) = 1$. At finite temperature this only holds approximately.

In summary we have derived that for appropriately chosen RG-schemes with $z = Z(\mu)$ the DSE for the Polyakov loop potential effectively boils down to a simple one-loop form, depicted in Fig. 14.

In Appendix B the one-loop diagrams in Fig. 14 are

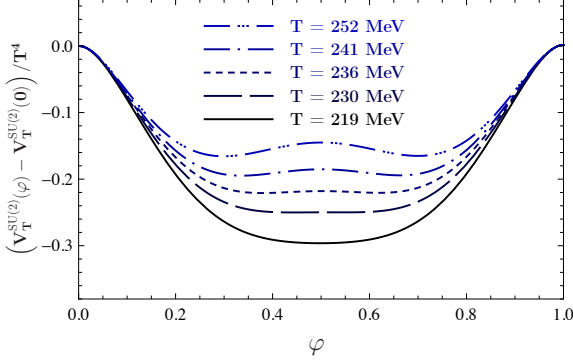


FIG. 15: Polyakov loop potential for $SU(2)$ from its DSE/2PI-representation within an optimised RG-scheme.

reduced to

$$V'(\varphi) = \frac{1}{2} V'_{\text{Weiss}}(\varphi) + \oint_q 2\pi T (n + \varphi) \times [z_a G_L(q + 2\pi T \varphi) + 2 z_a G_T(q + 2\pi T \varphi) - 2 z_c G_c(q + 2\pi T \varphi)], \quad (96)$$

where G_L , G_T , G_c are the propagators for the chromoelectric gluon, the chromomagnetic gluon and ghost propagators normalised $z_{a/c} = Z_{a/c}(\mu^2)$ at vanishing temperature at the point $p^2 = \mu^2$, and the first term originates in the gauge mode. The evaluation of (96) leads to the potential depicted in Fig. 15 for $SU(2)$ and Fig. 16 for $SU(3)$. From those the confinement-deconfinement critical temperature is determined at

$$T_c^{SU(2)} = 235 \pm 25 \text{ MeV} \quad \text{and} \quad T_c^{SU(3)} = 275 \pm 25 \text{ MeV}, \quad (97)$$

which gives

$$T_c^{SU(2)}/\sqrt{\sigma} \approx 0.56 \quad \text{and} \quad T_c^{SU(3)}/\sqrt{\sigma} \approx 0.655. \quad (98)$$

These results are in quantitative agreement with the FRG results, (78), and can be compared with lattice results in (81) and (82).

We close this chapter with a comparison of the temperature-dependence of the FRG and DSE/2PI potentials. Note that the DSE/2PI computation presented here approximately also takes into account the integrated RG-improvement in (86) for temperatures about the phase transition temperature. Hence, not only T_c but also the potentials themselves should agree quantitatively for temperatures close to T_c . We also remark that for $T \rightarrow 0$ the present approximation may lose its quantitative character as the normalisation of the ghost and gluon propagators changes rapidly for momenta $p^2 \approx (2\pi T)^2$ important for the Polyakov loop potential. In Fig. 17 we only show the comparison of the

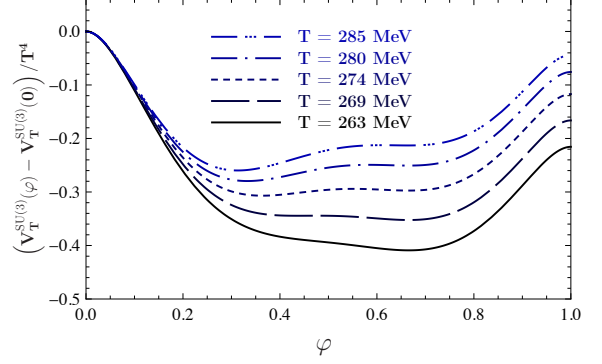


FIG. 16: Polyakov loop potential for $SU(3)$ from its DSE/2PI-approach within an optimised RG-scheme.

potentials for $SU(2)$, as that for $SU(3)$ simply follows from an weighted sum over $SU(2)$ -potentials, cf. Appendix B. The potentials agree quantitatively to a surprising level of accuracy which confirms the quantitative nature of both, FRG and DSE/2PI-computations. For temperatures $T/T_c \rightarrow 0$ there is a significant deviation as the DSE/2PI-approximations used here loses its quantitative nature. Note that this also holds for the approximation (40). In turn for $T/T_c \rightarrow \infty$ both approaches converge towards the perturbative potential. The present approximation in the DSE/2PI-approach is easily improved by taking into account the two-loop terms in (88). The discussion of the respective results goes beyond the scope of the present work and will be presented elsewhere.

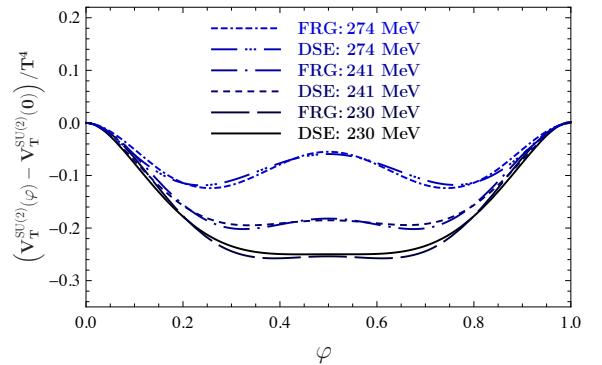


FIG. 17: Comparison of the Polyakov loop potential for $SU(2)$ from the DSE/2PI- with the FRG-approach.

VI. CONCLUSIONS

We have studied the confinement-deconfinement phase transition of static quarks with the effective potential of the Polyakov. The position of the minima signals the presence or absence of confinement, as they can be related to the free energy of a single quark. The potential itself was computed in the background field formalism in the Landau-deWitt gauge. This allows for the use of Landau gauge propagators at vanishing background, which had been obtained previously in the framework of the FRG [4–6]. The study here was done within different non-perturbative functional continuum approaches, i.e. using FRG-, DSE- and 2PI-representations of the effective action.

In all variants we find a second order phase transition for $SU(2)$ and a first order transition for $SU(3)$, as it is expected from lattice QCD. The corresponding temperatures agree quantitatively for all functional methods within the estimated error of approximately 10%, originating in the normalisation of the total momentum scale. The results including the lattice temperatures are summarised and discussed in Section V A and Section V B. These results are stable w.r.t. the choice of scaling or decoupling type solutions for the propagators and, furthermore, to the variation of the regulator in the FRG approach. The critical temperature for $SU(3)$ from functional methods agrees quantitatively with the corresponding lattice temperature. For $SU(2)$ the critical temperature from functional methods is significantly lower than the lattice temperature. This is linked to the missing back-reaction of the fluctuations of the Polyakov loop potential, see Section II B. Its inclusion leads to critical temperatures in quantitative agreement with the lattice results and the correct Ising-type critical scaling, see [2, 46].

The dependence of the Polyakov loop potential on the individual gluon and ghost modes is easily tractable. This was exploited to derive a simple criterion for static quark confinement. For infrared suppressed gluon but not suppressed ghost propagators confinement is imminent at sufficiently low temperatures. Independent of the functional approach chosen above, this is due to the fact, that the two non-suppressed confining ghost modes always overcompensate the deconfining trivial gluon gauge mode. As a result of their suppression, the remaining transversal gluon modes decouple at temperature scales far lower than the suppression scale and confinement is realised.

This confinement criterion has also been applied to general Yang–Mills-matter systems with matter in the adjoint and the fundamental representation. For matter in the adjoint representation again an infrared suppressed gluon is mandatory. Moreover, the criterion is sensitive to the difference between Higgs phase and confined phase even though both phases have infrared suppressed gluons. For matter in the fundamental representation the matter part of the potential breaks center symmetry. Hence

it is only possible to evaluate the relative importance of center symmetry modes and center breaking modes.

In summary the work establishes both on the qualitative and quantitative level the functional approach to confinement by means of the Polyakov loop potential. It only requires the computation and discussion of background-gauge propagators and hence allows a very simple access to structural questions such as the confinement mechanism as well to explicit analytic and numerical computations of the phase structure.

Acknowledgments — We thank Jens Braun, Astrid Eichhorn, Christian S. Fischer, Holger Gies, Jan Lücker and Axel Maas for discussions. This work is supported by the Helmholtz Alliance HA216/EMMI and by ERC-AdG-290623. LF is supported by the Science Foundation Ireland in respect of the Research Project 11-RFP.1-PHY3193 and the Helmholtz Young Investigator Grant VH-NG-322.

Appendix A: Regulators

The regulator function introduced in the FRG approach can be chosen freely as long as it fulfills certain limits. Firstly, it must have the same tensor structures as the corresponding two-point function. Neglecting those tensors for the moment, $R_k(p)$ must (i) regulate the propagator in the infrared, (ii) leave the full quantum theory for vanishing renormalisation group scale k and (iii) suppress fluctuations at large scales to reduce to the classical action. Formally, these requirements are met by

$$(i) \quad \lim_{p^2/k^2 \rightarrow 0} R_k(p) > 0, \quad (A1)$$

$$(ii) \quad \lim_{k^2/p^2 \rightarrow 0} R_k(p) = 0, \quad (A2)$$

$$(iii) \quad \lim_{k^2/p^2 \rightarrow \infty} R_k(p) \rightarrow \infty. \quad (A3)$$

The full theory is independent of the choice of $R_k(p)$, however, in truncations this may not be satisfied. This rules out certain forms of the regulator. Another restricting factor is the applicability in the computations, as some regulators are not feasible numerically.

For the thermal gluon and ghost propagators of Yang–Mills theory, four-dimensional exponential regulators,

$$R_{k,m}^{(0)}(p) = p^2 r_m(p^2/k^2) = p^2 \frac{(p^2/k^2)^{m-1}}{e^{(p^2/k^2)^m} - 1}, \quad (A4)$$

with $m = 2$, have proven to be well suited for numerical purposes [4–6]. Note however, that for the numerical computation of the Polyakov loop potential the regulator must not be too sharp, thus, $m \lesssim 2$, cf. [6].

The regulation of the propagator in the infrared demands that $R_k(p)$ is of approximately the same amplitude than the $\Gamma_k^{(2)}$ at each k . This is ensured by a pref-

actor such, that

$$R_{L/T/c,k,m}(p) = \bar{Z}_{L/T/c,k} R_{k,m}^{(0)}(p). \quad (\text{A5})$$

For the purpose presented here the precise form of \bar{Z} is not crucial but lengthy, thus, for the exact definitions we refer the interested reader to [4–6]. The results presented in section V A are obtained with regulators (A5).

In order to test the (in)dependence of the Polyakov loop potential on the choice of the regulator, we have studied different functions $R_k^{(0)}(p)$ and prefactors in the full regulator function. This was done for temperature-independent propagators, since not all choices of $R_k(p)$ are viable for thermal effects.

The scale-dependency of the propagators, of both scaling and decoupling type, was obtained with (A5) for $m = 1, 2$ [4–6]. These results were, firstly, combined with self-consistent choices in the determination of the Polyakov loop potentials. Secondly, the Polyakov loop potential was computed with these propagators but $R_k(p) = R_{k,m}^{(0)}(p)$ with $m = 1, 2$. Measured on the level of the confinement-deconfinement phase transition temperature of $SU(2)$, we find good stability w.r.t. the variation of the regulators and, furthermore, w.r.t. scaling of decoupling type propagators, as all choices are within 5% deviation. Furthermore, we found that for different choices of the regulator in propagators and Polyakov loop potential, namely those which have relative shifts in the renormalisation group scale, the truncation effects may grow larger.

Appendix B: One-Loop Diagrams in the DSE for the Polyakov Loop Potential

The one-loop diagrams are given in Fig. 14. Both couple the external temporal gluonic background to the fluctuating loop fields. For clarity we consider temperature-independent propagators first, before we decompose the tensor structures for the case of non-trivial temperature dependence of the propagators.

The gluon loop, depicted in Fig. 18(a), involves the three-gluon vertex with one background leg. At vanishing fields it is given by

$$(S_{A_0aa}^{(3)})_{\rho\mu\nu} = (S_{aaa}^{(3)})_{\rho\mu\nu} + \frac{1}{\xi} \frac{\delta(\bar{D}_\mu \bar{D}_\nu)}{\delta A_0}, \quad (\text{B1})$$

where the second term originates from the background field dependence of the gauge fixing term, see (5). The classical vertex is given in Fig. 18(b). For this very definition it is given by

$$(S_{aaa}^{(3)})_{\mu\nu\rho}^{abc}(p, q, k) = igf^{abc} (\delta_{\mu\nu}(p-q)_\rho + \delta_{\nu\rho}(q-k)_\mu + \delta_{\rho\mu}(k-p)_\nu). \quad (\text{B2})$$

At $T = 0$ the gluon propagator has four degrees of

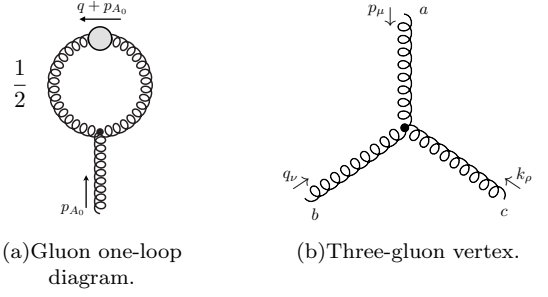


FIG. 18: Gluon one-loop diagram in the DSE for the Polyakov loop potential.

freedom, three transversal modes and the longitudinal gauge mode, thus, at vanishing fluctuation fields and a constant background we can split the gluon propagator according to

$$(G_A)_{\mu\nu} = (G_A^\perp)_{\mu\nu} + \xi \bar{D}_\mu \frac{1}{\bar{D}^2} \bar{D}_\nu, \quad (\text{B3})$$

where the first term is the non-trivial transversal part $\bar{D}_\mu (G_A^\perp)_{\mu\nu} = 0$, whereas the second term represents the gauge mode. This is a consequence of the corresponding Slavnov–Taylor identities: The quantum corrections to the propagator are transversal and, hence, the gauge sector is unchanged. Together with the background vertex (B1) this leaves us with a contribution of the gauge sector

$$\frac{1}{2} \text{Tr} \left\{ \frac{1}{\xi} \frac{\delta(\bar{D}_\mu \bar{D}_\nu)}{\delta \bar{A}_\rho} \xi \bar{D}_\nu \frac{1}{\bar{D}^2} \bar{D}_\mu \right\} = \frac{\delta}{\delta \bar{A}_\rho} \frac{1}{2} \text{Tr} \log(-\bar{D}^2), \quad (\text{B4})$$

where the trace on the right hand side does not include a trace over Lorentz indices and gives $1/2 V_{\text{Weiss}}$, the perturbative one-loop potential. The latter is given by

$$V_{SU(N_c)}^{\text{Weiss}} = -\frac{d-2}{\pi^{d/2}} \Gamma(d/2) T^d \sum_{l=1}^{N_c^2-1} \sum_{n=1}^{\infty} \frac{\cos\{2\pi n \nu_l |\varphi|\}}{n^d}, \quad (\text{B5})$$

where d is the number of spacetime dimensions and ν_l are the eigenvalues of the generators of the gauge group spanned via the Cartan subalgebra. For $SU(2)$ the eigenvalues are $\nu_l = 0, 1, -1$. For $SU(3)$ and the background-independent propagators one can construct the potential according to the eigenvalues,

$$V_{SU(3)}(\varphi^3, \varphi^8) = V_{SU(2)}(\varphi^3) + V_{SU(2)}\left(\frac{\varphi^3 + 3\sqrt{\varphi^8}}{2}\right) + V_{SU(2)}\left(\frac{\varphi^3 - 3\sqrt{\varphi^8}}{2}\right). \quad (\text{B6})$$

The non-trivial part of the computation concerns the transversal part $(G_a^\perp)_{\mu\nu}(p) = G_a^\perp(p) \Pi_{\mu\nu}^\perp(p)$, which cou-

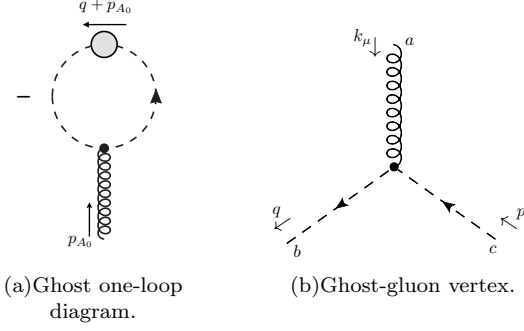


FIG. 19: Ghost one-loop diagram in the DSE for the Polyakov loop potential.

ples to the standard part of the three-gluon vertex, $S_{aaa}^{(3)}$, given in (B2). Note that at vanishing temperature the propagator is $O(4)$ -symmetric, thus, it only depends on the absolute value of the momentum, not on the spatial and temporal components separately like at non-vanishing temperature, see (11).

For a purely temporal momentum p_{A_0} the loop diagram in Fig. 18(a) translates to

$$\begin{aligned} & \frac{1}{2} \oint_q z_a (G_a^\perp)_{\mu\nu}(p_{A_0} + q) (S_{aaa}^{(3)})_{0\mu\nu}(p_{A_0}, p_{A_0} + q, -p_{A_0} - q) \\ &= ig \oint_q z_a G_a^\perp(p_{A_0} + q) (p_{A_0} + q)_\rho (\delta_{\mu\mu} - 1), \end{aligned} \quad (B7)$$

where due to symmetry only the term $\propto p_{A_0} + q_0 = 2\pi T(n_q + \varphi)$ survives, with $q_0 = 2\pi T n_q$ and z_a according to (30).

In (B7) the factor $(\delta_{\mu\mu} - 1)$ counts the three coinciding transversal modes. For thermal propagators the projection is such, that it accounts for the chromoelectric and chromomagnetic modes. Thus, without repeating the computation along the lines of (B7), we get the final expression for the loop diagram Fig. 18(a) as

$$\begin{aligned} & ig \oint_q 2\pi T(n_q + \varphi) (z_a G_L(2\pi T(n_q + \varphi), \vec{q}) \\ & + 2z_a G_T(2\pi T(n_q + \varphi), \vec{q})), \end{aligned} \quad (B8)$$

with G_L and G_T being the chromoelectric and chromomagnetic gluon propagators with the normalisation at vanishing temperature given in (30).

Having the similar structure as the gluon loop, the ghost loop is given in Fig. 19(a). The first ingredient of this diagram is the classical ghost-gluon vertex as defined in Fig. 19(b). It is given by

$$(S_{A_0 c \bar{c}}^{(3)})_{\mu}^{abc}(0, q, p) = 2 (S_{ac \bar{c}}^{(3)})_{\mu}^{abc}(0, q, p) = 2ig f^{abc} q_{\mu}. \quad (B9)$$

Note that the ghost-gluon vertex involves an additional factor of 2 compared to the vertex in standard Landau gauge, due to the appearance of the covariant derivative

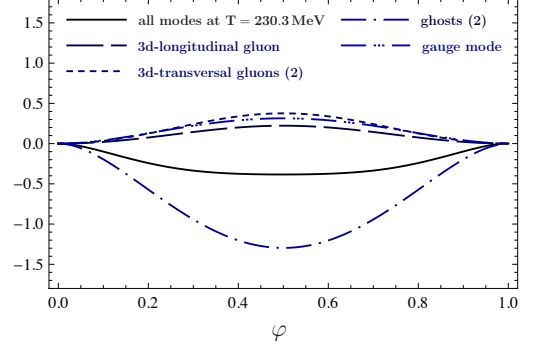


FIG. 20: Contributions from individual modes to the Polyakov loop potential.

\bar{D}_μ (instead of a plain derivative ∂_μ) in the last term of (5).

The second component in the ghost loop is the full ghost propagator. It is a Lorentz scalar, thus, dropping the colour structure it is simply given by a scalar function $G_c(p_0, \vec{p})$. Thus, for trivial and non-trivial implicit temperature dependence of the propagator, the diagram attached to a purely temporal gluon field in Fig. 19(a) reduces to

$$\begin{aligned} & - \oint_q z_c G_c((p_{A_0})_0 + q_0, \vec{q}) (S_{Ac\bar{c}}^{(3)})_{\rho}(p_{A_0} + q, p_{A_0}, -p_{A_0} - q) \\ &= -2ig \oint_q z_c G_c((p_{A_0})_0 + q_0, \vec{q}) (p_{A_0} + q)_{\mu}, \end{aligned} \quad (B10)$$

where $z_c = z_c(\mu)$. Due to symmetry, this only leaves the term

$$-2ig \oint_q z_c G_c(2\pi T(n_q + \varphi), \vec{q}) 2\pi T(n_q + \varphi). \quad (B11)$$

In combination with the gauge mode, the sum of the individual contributions yields the final expression for the DSE of the Polyakov loop potential (96).

Due to the different sign in the ghost loop and the gluon suppression the potential shows confinement for small temperatures. The additive contributions of the different modes, the chromoelectric, chromomagnetic, gauge modes from the gluon and the ghost modes, are illustrated in Fig. 20 at a temperature around the phase transition. For lower temperatures, the ghost contributions grow stronger and the transverse gluons decrease further. In contrast, for higher temperatures the propagator approach the perturbative forms, thus, the potential approaches the (deconfining) Weiss potential (B5).

Appendix C: Confinement for Mildly Suppressed Gluons

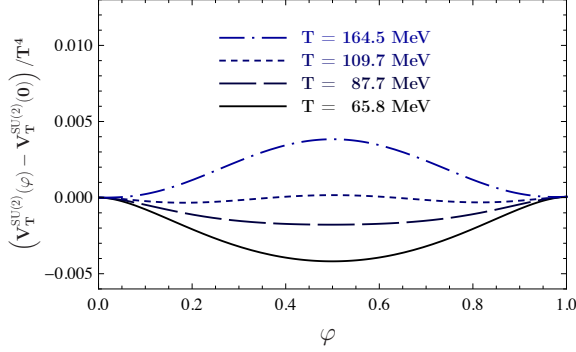


FIG. 21: The Polyakov loop potential from its DSE for mildly suppressed transversal gluons and trivial ghosts shows confinement for sufficiently low temperatures.

In this section we confirm the hypothesis made in section III in a numerical application for both approaches DSEs and the FRG. In these computations the ghosts are left trivial, thus, they give a confining potential which overcompensates the gauge mode, and both terms sum up to $-1/2V_{\text{Weiss}}$. We show, that already a soft suppression of transversal gluons yields a decrease of the deconfining effect such, that confinement is immanent at sufficiently low temperatures.

For the DSE we choose an ansatz, in which transversal gluons are suppressed for infrared momenta, thus,

$$\Gamma_a^{(2)}(p^2) = p^2 (1 + (p^2)^{\kappa_a}), \text{ with } \kappa_a = -0.2. \quad (\text{C1})$$

The full result is given in Fig. 21, where clearly a confining potential is realised at low temperatures.

In the case of the FRG the suppression must also be present in the renormalisation group flow along the scale k . Thus, a qualified ansatz is given by

$$\Gamma_{a,k}^{(2)}(p^2) = (p^2 + k^2)^{1+\kappa_a}, \text{ with } \kappa_a = -0.2. \quad (\text{C2})$$

The result for this ansatz is given in Fig. 22.

From these two examples we can infer, that indeed a mild gluon suppression is sufficient to yield a confining potential at low temperatures, as we claimed in section III. Nevertheless, the sum of gluonic, ghost and gauge modes is non-trivial, thus, we refrain from giving phase transition temperatures here, as these examples only serve as a proof of principle and are of no quantitative physical relevance.

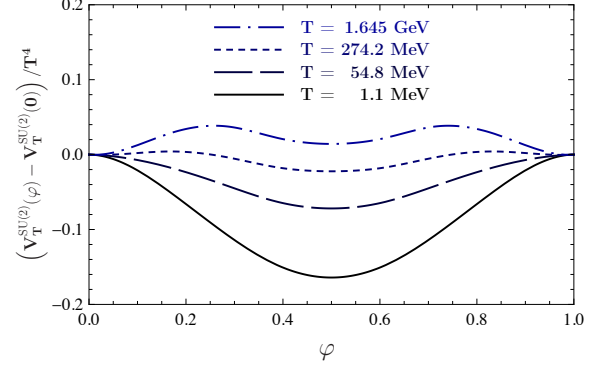


FIG. 22: The Polyakov loop potential from its FRG equation for mildly suppressed transversal gluons and trivial ghosts shows confinement for sufficiently low temperatures.

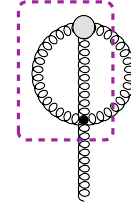


FIG. 23: Three gluon vertex correction from the two-loop diagram

Appendix D: Direct resummation of the DSE-hierarchy

In this appendix we provide the necessary steps for deriving (84) solely within the DSE-approach. Note that this simply amounts to using the ghost and gluon gap equations in the DSE hierarchy which is trivially implemented in the 2PI-approach. To that end we have to rewrite the two-loop diagrams in (27), Fig. 2. Similarly to the 2PI argument leading to (84) this diagram can be turned into a one-loop form within a resuma-

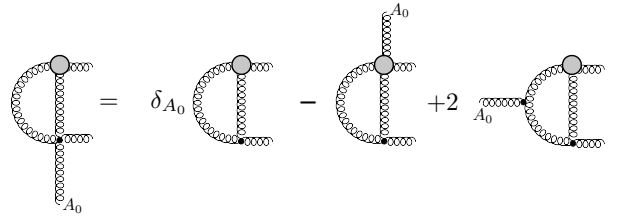


FIG. 24: Approximation of the substructure of the dashed box in Fig. 23.

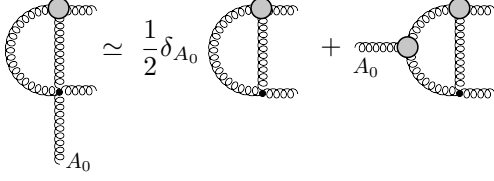


FIG. 25: Approximation for the three-gluon vertex of Fig. 24.

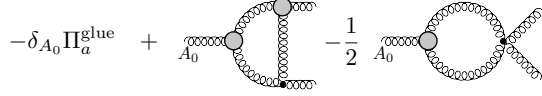


FIG. 26: Identification of the gluon vacuum polarisation in the two-loop diagram of the DSE.

tion scheme which neglects some order α_s^2 -corrections to full vertices but takes into account full propagators. In the following we explicitly perform this analysis for the gluon two-loop diagram, the same steps can be trivially taken over for the ghost two-loop diagram: First, we note that the two-loop diagram has no contributions from the gauge fixing vertices proportional to $1/\xi$ which contributes in the one-loop diagram, see Appendix B. The reason is that the full and renormalised classical vertices involve more than 2 fluctuating fields a . Moreover, the two-loop contribution can be seen as a vertex-correction diagram to the gluonic one-loop diagram, see Fig. 23.

The vertex correction can be rewritten in terms of a

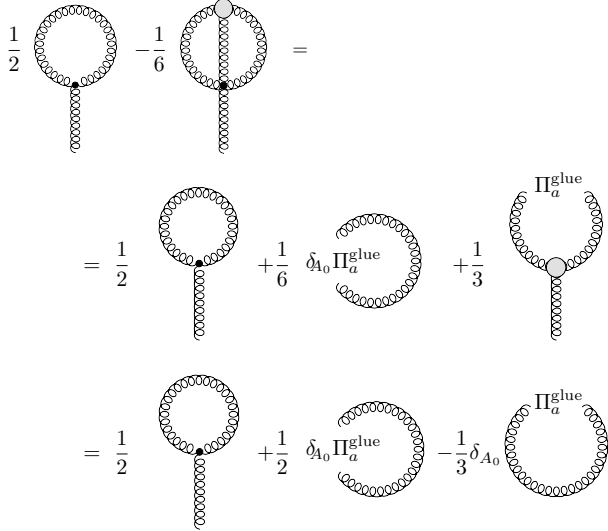


FIG. 27: Approximation of glue part of the DSE for the Polyakov loop potential.

total A_0 -derivative, a three-gluon vertex diagram and a term which resembles (minus) the vertex correction, see Fig. 24. The only difference is that the A_0 leg is attached to the full vertex. Since the two fluctuating fields are attached to the additional propagator in the two-loop diagram, the original diagram and this one differ in order α_s^2 in the vertex. Hence, in the present approximation we identify it with (minus) the vertex correction. We also note that strictly speaking the last diagram in Fig. 24 only involves the A_0 -vertex originating in S_A . However, the gauge fixing part does not contribute anyway as the vertex is contracted with two transversal propagators. Hence, for the sake of simplicity we will always use the full A_0 -vertices, but the gauge-part is projected out in the diagrams.

Moving the vertex correction to the left hand side leads to the form Fig. 25 of the vertex correction, up to the vertex correction-terms of order α_s^2 . The first term on the right hand side of Fig. 25 is (minus) the three-gluon vertex part of the gluonic part Π_a^{glue} of the gluon vacuum polarisation Π_a , see Fig. 10. We rewrite it accordingly and the right hand side takes the form displayed in Fig. 26,

$$-\frac{1}{3}\partial_{A_0}\Pi_a^{\text{glue}} + \text{diagrams}. \quad (\text{D1})$$

Upon closing the open a -lines in Fig. 26 with the remaining gluon propagator the corresponding one-loop sub-diagrams constitute Π_a^{glue} up to a factor $1/2$ in the tadpole diagram. As for the 2PI-derivation we drop this diagram. Inserting Fig. 26 into Fig. 23 we are led to Fig. 27.

Similar steps as above can be done for the ghost two-loop diagram. Here we simply note that the two ghost terms in the DSE Fig. 2 can be rewritten as displayed in Fig. 28. The first term on the rhs in Fig. 28 is the A_0 -derivative of the $\text{Tr} \log G_c$ -term in (84). In turn, the two remaining terms equal

$$\frac{\delta}{\delta \bar{A}_0} \left[-\frac{2}{3} \left(\frac{1}{2} \text{Tr} \Pi_a^{\text{ghost}} G_a - \text{Tr} \Pi_c G_c \right) + O(\alpha_s^2) \right]. \quad (\text{D2})$$

This is most easily seen by just comparing the perturbative two-loop diagrams in both expressions.

In summary the gluonic and ghost terms in the DSE add up to the total A_0 -derivative (84).

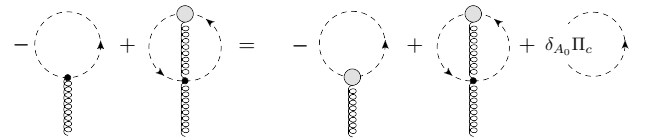


FIG. 28: Approximation of ghost part of the DSE for the Polyakov loop potential.

-
- [1] J. Braun, H. Gies, and J. M. Pawłowski, *Phys.Lett. B* **684**, 262 (2010), 0708.2413.
 - [2] F. Marhauser and J. M. Pawłowski, (2008), 0812.1144.
 - [3] J. Braun, A. Eichhorn, H. Gies, and J. M. Pawłowski, *Eur.Phys.J. C* **70**, 689 (2010), 1007.2619.
 - [4] L. Fister and J. M. Pawłowski, (2011), 1112.5440.
 - [5] L. Fister and J. M. Pawłowski, (2011), 1112.5429.
 - [6] L. Fister, PhD thesis, Heidelberg University (2012).
 - [7] R. Alkofer and L. von Smekal, *Phys. Rept.* **353**, 281 (2001), hep-ph/0007355.
 - [8] C. D. Roberts and S. M. Schmidt, *Prog. Part. Nucl. Phys.* **45**, S1 (2000), nucl-th/0005064.
 - [9] C. S. Fischer, *J.Phys.G* **G32**, R253 (2006), hep-ph/0605173.
 - [10] C. S. Fischer, A. Maas, and J. M. Pawłowski, *Annals Phys.* **324**, 2408 (2009), 0810.1987.
 - [11] D. Binosi and J. Papavassiliou, *Phys.Rept.* **479**, 1 (2009), 0909.2536.
 - [12] J. M. Pawłowski, *AIP Conf.Proc.* **1343**, 75 (2011), 1012.5075.
 - [13] A. Maas, *Phys. Rep. in press* (2013), 1106.3942.
 - [14] L. von Smekal, *Nucl.Phys.Proc.Suppl.* **228**, 179 (2012), 1205.4205.
 - [15] J. Braun, L. M. Haas, F. Marhauser, and J. M. Pawłowski, *Phys.Rev.Lett.* **106**, 022002 (2011), 0908.0008.
 - [16] C. Gatttringer, *Phys. Rev. Lett.* **97**, 032003 (2006), hep-lat/0605018.
 - [17] F. Synatschke, A. Wipf, and C. Wozar, *Phys.Rev. D* **75**, 114003 (2007), hep-lat/0703018.
 - [18] E. Bilgici, F. Bruckmann, C. Gatttringer, and C. Hagen, *Phys.Rev. D* **77**, 094007 (2008), 0801.4051.
 - [19] C. S. Fischer, *Phys. Rev. Lett.* **103**, 052003 (2009), 0904.2700.
 - [20] C. S. Fischer and J. A. Mueller, *Phys. Rev. D* **80**, 074029 (2009), 0908.0007.
 - [21] C. S. Fischer, J. Luecker, and J. A. Mueller, *Phys.Lett. B* **702**, 438 (2011), 1104.1564.
 - [22] C. S. Fischer and J. Luecker, *Phys.Lett. B* **718**, 1036 (2013), 1206.5191.
 - [23] M. Hopfer, M. Mitter, B.-J. Schaefer, and R. Alkofer, (2012), 1211.0166.
 - [24] A. Eichhorn, (2011), 1111.1237.
 - [25] H. Reinhardt and J. Heffner, *Phys.Lett. B* **718**, 672 (2012), 1210.1742.
 - [26] D. Diakonov, C. Gatttringer, and H.-P. Schadler, *JHEP* **1208**, 128 (2012), 1205.4768.
 - [27] J. Greensite, *Phys.Rev. D* **86**, 114507 (2012), 1209.5697.
 - [28] K. Fukushima and K. Kashiwa, (2012), 1206.0685.
 - [29] K. Kashiwa and Y. Maezawa, (2012), 1212.2184.
 - [30] A. Cucchieri, A. Maas, and T. Mendes, *Phys. Rev. D* **75**, 076003 (2007), hep-lat/0702022.
 - [31] C. S. Fischer, A. Maas, and J. A. Müller, *Eur. Phys. J. C* **68**, 165 (2010), 1003.1960.
 - [32] A. Maas, J. M. Pawłowski, L. von Smekal, and D. Spielmann, *Phys.Rev. D* **85**, 034037 (2012), 1110.6340.
 - [33] V. Bornyakov and V. Mitrjushkin, *Int.J.Mod.Phys. A* **27**, 1250050 (2012), 1103.0442.
 - [34] A. Cucchieri and T. Mendes, *PoS FACESQCD*, 007 (2010), 1105.0176.
 - [35] R. Aouane *et al.*, *Phys.Rev. D* **85**, 034501 (2012), 1108.1735.
 - [36] R. Aouane, F. Burger, E.-M. Ilgenfritz, M. Muller-Preussker, and A. Sternbeck, (2012), 1212.1102.
 - [37] A. Maas, J. Wambach, B. Grüter, and R. Alkofer, *Eur. Phys. J. C* **37**, 335 (2004), hep-ph/0408074.
 - [38] B. Gruter, R. Alkofer, A. Maas, and J. Wambach, *Eur.Phys.J. C* **42**, 109 (2005), hep-ph/0408282.
 - [39] A. Maas, J. Wambach, and R. Alkofer, *Eur. Phys. J. C* **42**, 93 (2005), hep-ph/0504019.
 - [40] L. Abbott, *Nucl.Phys. B* **185**, 189 (1981).
 - [41] N. K. Nielsen, *Nucl. Phys. B* **101**, 173 (1975).
 - [42] J. M. Pawłowski, *Int.J.Mod.Phys. A* **16**, 2105 (2001).
 - [43] D. F. Litim and J. M. Pawłowski, *JHEP* **0209**, 049 (2002), hep-th/0203005.
 - [44] J. M. Pawłowski, (2003), hep-th/0310018.
 - [45] J. M. Pawłowski, *Annals Phys.* **322**, 2831 (2007), hep-th/0512261.
 - [46] F. Spallek, Diploma thesis, Heidelberg University (2010).
 - [47] D. F. Litim and J. M. Pawłowski, *World Sci.*, 168 (1999), hep-th/9901063.
 - [48] J. Berges, N. Tetradis, and C. Wetterich, *Phys. Rept.* **363**, 223 (2002), hep-ph/0005122.
 - [49] J. Polonyi, *Central Eur.J.Phys.* **1**, 1 (2003), hep-th/0110026.
 - [50] H. Gies, (2006), hep-ph/0611146.
 - [51] B.-J. Schaefer and J. Wambach, *Phys.Part.Nucl.* **39**, 1025 (2008), hep-ph/0611191.
 - [52] Y. Igarashi, K. Itoh, and H. Sonoda, *Prog.Theor.Phys.Suppl.* **181**, 1 (2010), 0909.0327.
 - [53] O. J. Rosten, *Phys.Rept.* **511**, 177 (2012), 1003.1366.
 - [54] J. Braun, *J.Phys. G* **39**, 033001 (2012), 1108.4449.
 - [55] J. C. Taylor, *Nucl. Phys. B* **33**, 436 (1971).
 - [56] C. Lerche and L. von Smekal, *Phys. Rev. D* **65**, 125006 (2002), hep-ph/0202194.
 - [57] J. M. Luttinger and J. C. Ward, *Phys. Rev.* **118**, 1417 (1960).
 - [58] T. Lee and C. Yang, *Phys.Rev.* **117**, 22 (1960).
 - [59] G. Baym, *Phys.Rev.* **127**, 1391 (1962).
 - [60] C. de Dominicis and P. C. Martin, *J.Math.Phys.* **5**, 14 (1964).
 - [61] J. M. Cornwall, R. Jackiw, and E. Tomboulis, *Phys. Rev. D* **10**, 2428 (1974).
 - [62] J. Blaizot, E. Iancu, and A. Rebhan, *Phys.Rev.Lett.* **83**, 2906 (1999), hep-ph/9906340.
 - [63] J. Blaizot, E. Iancu, and A. Rebhan, *Phys.Lett. B* **470**, 181 (1999), hep-ph/9910309.
 - [64] J. Blaizot, E. Iancu, and A. Rebhan, *Phys.Rev. D* **63**, 065003 (2001), hep-ph/0005003.
 - [65] E. Braaten and E. Petitgirard, *Phys.Rev. D* **65**, 085039 (2002), hep-ph/0107118.
 - [66] A. Arrizabalaga and J. Smit, *Phys.Rev. D* **66**, 065014 (2002), hep-ph/0207044.
 - [67] E. Mottola, (2003), hep-ph/0304279.
 - [68] M. E. Carrington, G. Kunstatler, and H. Zaraket, *Eur. Phys. J. C* **42**, 253 (2005), hep-ph/0309084.
 - [69] J. Berges, *Phys.Rev. D* **70**, 105010 (2004), hep-ph/0401172.
 - [70] J. O. Andersen and M. Strickland, *Phys.Rev. D* **71**, 025011 (2005), hep-ph/0406163.
 - [71] M. Carrington and E. Kovalchuk, *Phys.Rev. D* **76**, 1108.1735.

- 045019 (2007), 0705.0162.
- [72] U. Reinosa and J. Serreau, *JHEP* **0711**, 097 (2007), 0708.0971.
 - [73] U. Reinosa and J. Serreau, *Nucl.Phys.* **A820**, 139C (2009), 0810.4883.
 - [74] U. Reinosa and J. Serreau, *Annals Phys.* **325**, 969 (2010), 0906.2881.
 - [75] J.-P. Blaizot, J. M. Pawłowski, and U. Reinosa, *Phys.Lett.* **B696**, 523 (2011), 1009.6048.
 - [76] M. Carrington, (2012), 1211.4127.
 - [77] C. S. Fischer and J. M. Pawłowski, *Phys. Rev.* **D75**, 025012 (2007), hep-th/0609009.
 - [78] C. S. Fischer and J. M. Pawłowski, *Phys. Rev.* **D80**, 025023 (2009), 0903.2193.
 - [79] D. Zwanziger, *Phys. Rev.* **D65**, 094039 (2002), hep-th/0109224.
 - [80] J. M. Pawłowski, D. F. Litim, S. Nedelko, and L. von Smekal, *Phys. Rev. Lett.* **93**, 152002 (2004), hep-th/0312324.
 - [81] J. Braun and A. Janot, *Phys.Rev.* **D84**, 114022 (2011), 1102.4841.
 - [82] J. Braun and T. K. Herbst, (2012), 1205.0779.
 - [83] L. Fister, (2010), 1002.1649.
 - [84] L. Fister, R. Alkofer, and K. Schwenzer, *Phys.Lett.* **B688**, 237 (2010), 1003.1668.
 - [85] V. Macher, Diploma thesis, University of Graz (2010).
 - [86] R. Alkofer, L. Fister, A. Maas, and V. Macher, *AIP Conf.Proc.* **1343**, 179 (2011), 1011.5831.
 - [87] V. Macher, A. Maas, and R. Alkofer, *Int.J.Mod.Phys.* **A27**, 1250098 (2012), 1106.5381.
 - [88] N. Weiss, *Phys.Rev.* **D24**, 475 (1981).
 - [89] D. J. Gross, R. D. Pisarski, and L. G. Yaffe, *Rev.Mod.Phys.* **53**, 43 (1981).
 - [90] K. Osterwalder and E. Seiler, *Annals Phys.* **110**, 440 (1978).
 - [91] E. H. Fradkin and S. H. Shenker, *Phys. Rev.* **D19**, 3682 (1979).
 - [92] J. Kertész, *Physica A* **161**, 58 (1989).
 - [93] I. Boettcher, J. M. Pawłowski, and S. Diehl, *Nucl.Phys.Proc.Suppl.* **228**, 63 (2012), 1204.4394.
 - [94] I. Boettcher, S. Diehl, J. M. Pawłowski, and C. Wetterich, (2012), 1209.5641.
 - [95] B. Lucini and M. Panero, (2012), 1210.4997.
 - [96] P. N. Meisinger and M. C. Ogilvie, *Phys.Lett.* **B379**, 163 (1996), hep-lat/9512011.
 - [97] R. D. Pisarski, *Phys.Rev.* **D62**, 111501 (2000), hep-ph/0006205.
 - [98] K. Fukushima, *Phys.Lett.* **B591**, 277 (2004), hep-ph/0310121.
 - [99] A. Mocsy, F. Sannino, and K. Tuominen, *Phys.Rev.Lett.* **92**, 182302 (2004), hep-ph/0308135.
 - [100] A. Dumitru, Y. Hatta, J. Lenaghan, K. Orginos, and R. D. Pisarski, *Phys.Rev.* **D70**, 034511 (2004), hep-th/0311223.
 - [101] C. Ratti, M. A. Thaler, and W. Weise, *Phys.Rev.* **D73**, 014019 (2006), hep-ph/0506234.
 - [102] S. K. Ghosh, T. K. Mukherjee, M. G. Mustafa, and R. Ray, *Phys.Rev.* **D73**, 114007 (2006), hep-ph/0603050.
 - [103] B.-J. Schaefer, J. M. Pawłowski, and J. Wambach, *Phys.Rev.* **D76**, 074023 (2007), 0704.3234.
 - [104] Y. Sakai, K. Kashiwa, H. Kouno, and M. Yahiro, *Phys.Rev.* **D77**, 051901 (2008), 0801.0034.
 - [105] V. Skokov, B. Stokic, B. Friman, and K. Redlich, *Phys.Rev.* **C82**, 015206 (2010), 1004.2665.
 - [106] T. K. Herbst, J. M. Pawłowski, and B.-J. Schaefer, *Phys.Lett.* **B696**, 58 (2011), 1008.0081.